

AD-A282 340



①

**A NEW APPROACH TO VALIDATE SUBGRID MODELS  
IN COMPLEX HIGH REYNOLDS NUMBER FLOWS**

**Semi-Annual Report for the Period**

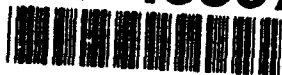
**October, 1993 - May, 1994**

**Grant Number: N00014-93-1-0342**

**DTIC  
ELECTE  
JUL 15 1994  
S G D**

**Suresh Menon  
School of Aerospace Engineering  
Georgia Institute of Technology  
Atlanta, Georgia 30332-0150**

**94-18867**



*4986*

**Submitted to  
Office of Naval Research**

Statement A per telecon Lawrence Purtell  
Office of the Chief of Naval Research  
800 north Quincy Street  
Arlington, VA 22217-5000  
NWW 7/8/94

Accession For	
NTIS CRA&I	<input checked="" type="checkbox"/>
DTIC TAB	<input type="checkbox"/>
Unannounced	<input type="checkbox"/>
Justification	
By	
Distribution /	
Availability Codes	
Dist	Avail and/or Special
A-1	

**94 6 17 030**

# **A NEW APPROACH TO VALIDATE SUBGRID MODELS IN COMPLEX HIGH REYNOLDS NUMBER FLOWS**

**Semi-Annual Report for the Period: October, 1993 - May, 1994**  
**Grant Number: N00014-93-1-0342**

**Suresh Menon**  
**School of Aerospace Engineering**  
**Georgia Institute of Technology**  
**Atlanta, Georgia 30332-0150**

## **1. INTRODUCTION**

This second semi-annual report summarizes the progress made in the last six months. The overall objectives of this research are to develop new methods to evaluate subgrid models and then to utilize these methods to improve the chosen subgrid models. The subgrid models investigated in this research are chosen primarily for application in high Reynolds number complex flows. Preliminary studies of these models have been completed. *A priori* analysis using data from direct numerical simulations (DNS) homogeneous isotropic flows was carried out, and then the models were implemented in large-eddy simulation (LES) codes and further evaluated. Two types of analysis methods have been developed so far. The first method uses information in Fourier (spectral) space and evaluates the interscale energy transfer as a function of the wavenumbers resolved in the LES. The second, uses information in the physical space and uses cross correlation analysis to investigate the behavior of subgrid models. The physical space analysis method will be the primary analysis tool for the next year's study, since the next phase of research will focus on complex flows such as flows past rearward facing steps and swirling flows.

In the following, we discuss recent developments of the last six months. Some of the results have been described in more detail in the papers (Menon and Yeung, 1994a, 1994b; Kim et al., 1994) and, therefore, will not be repeated here. These papers (or the extended abstracts) are included as appendices to this report.

## **2. ANALYSIS OF SUBGRID MODELS USING DNS AND LES OF ISOTROPIC TURBULENCE**

In this phase of research, homogeneous isotropic turbulence was used as a test flow field to develop analysis methods. This was motivated by the fact that isotropic turbulence has been studied extensively in the past and detailed DNS data is available. In addition, the computational domain is very simple and therefore, methods using spectral techniques can be used to identify features of the flow which are not possible using physical space methods and vice versa. Both incompressible and compressible isotropic fields have been studied using two different finite difference codes. These codes have been validated by comparing the DNS predictions by these codes with the results obtained using the well know spectral code of Rogallo.

## 2.1 Analysis of Incompressible Isotropic Turbulence

Various subgrid models were evaluated in both spectral and physical space using high resolution DNS data. Subsequently, these models were implemented in coarse grid LES. The spectral space method was used primarily for *a priori* analysis while the physical space method was used for both *a priori* and *posteriori* analysis. For *a priori* analysis, very high resolution data (using  $128^3$  grid) was used. All the *posteriori* analysis were carried out using LES data and without using any DNS information. This approach is essential for future application to high Reynolds number flows since DNS data for such flows will not be available.

For the physical space analysis of the subgrid models, LES using different grid resolutions is first carried out. Then, using top hat filtering, the modeled subgrid stresses and the energy transfer are correlated between the two LES data fields. For example, LES was carried out using  $32^3$  grid and  $16^3$  grid using identical initial flow field and using the same subgrid model. Then, at a chosen instant, the resolved field in the  $32^3$  grid is filtered to compute the subgrid stresses and energy transfer in the  $16^3$  grid. This field is considered 'exact', as far as the coarser grid is concerned, since the length scales that are unresolved (and hence modeled) in the coarser grid are supposed to be resolved in the finer grid LES. Therefore, if the model is working properly this 'exact' field must be reproduced by the subgrid model in the  $16 \times 16 \times 16$  grid. Cross correlation analysis between the modeled and 'exact' subgrid stresses and the energy transfer was carried out. If the correlation is high, it would suggest that the subgrid model behaves consistently for different grid resolutions and that the subgrid energy transfer is modeled correctly in the  $16 \times 16 \times 16$  LES. With this approach, model validation does not require DNS data and, more importantly, since the same flow field is being investigated, the model can be investigated directly in the flow field and geometry of interest. Furthermore, this approach allows an immediate assessment of the capability of the subgrid models in the coarsest grid.

Note that, the results of the above analysis methods do not provide any information on the accuracy of the results. Comparison with experimental data (or DNS data, where ever possible) is essential to demonstrate the accuracy of the LES. So far, for isotropic flows, DNS data have been used to evaluate the accuracy of the LES results, but future studies will be directed to more complex flows for which no DNS data is available. Comparison with experimental data will have to be carried out in such cases. It is expected that the analysis methods for model validation will also have to be further developed for complex flows, for example, to handle the near wall effects.

Various subgrid models have been implemented and evaluated using the techniques described above. More details of the analysis methods are given in Menon and Yeung (1994a, 1994b). The subgrid models studied so far are:

- (a) the classical Smagorinsky's eddy viscosity model
- (b) the dynamic (Germano's) eddy viscosity model
- (c) a spectral eddy viscosity model
- (d) a new scale similarity model
- (e) a one-equation model for the subgrid kinetic energy with and without stochastic backscatter
- (f) a dynamic one-equation model for the subgrid kinetic energy
- (g) a two-equation model for the subgrid kinetic energy and subgrid helicity (k-h model)

Smagorinsky's model is very popular in literature; however, it has been shown to require significant modifications (primarily adjustment of the 'constant') for good agreement with experimental data. The major 'breakthrough' in subgrid model development is the application of the algebraic identity of Germano to evaluate dynamically the constant in Smagorinsky's model. In Menon and Yeung (1994a), we studied the classical model with fixed constant while in Menon and Yeung (1994b) and Kim et al. (1994), we studied the dynamic eddy viscosity model.

The scale similarity model is a modified version of the original Bardina's model and was proposed by Meneveau (Liu et al., 1993) based on analysis of high Reynolds number experimental data on turbulent jets. It is based on the idea that the energy transfer at the resolved grid resolution is self similar to the energy transfer occurring at a resolution twice as coarse. This method, therefore, uses a test filter (an approach very similar to Germano's) to compute the scale-similar subgrid stresses in terms of the resolved field. Computationally, this model is very simple and easy to implement. However, as discussed in Menon and Yeung (1994a), there are some inherent limitations to this model when used in LES. This model can predict backscatter but the amount of backscatter may exceed the real backscatter. This can result in numerical instability and, therefore, some sort of backscatter control is necessary. More details of the analysis of this model are given below and in Menon and Yeung, (1994a).

The one equation model for the subgrid kinetic energy (k-equation model) was chosen keeping in mind the requirements for practical high Reynolds number LES. It is expected that for high Reynolds number LES of complex flows, the grid resolution practically possible (due to resource constraints) will be limited. Therefore, simple dissipative models (even with dynamic evaluations) may not be sufficient for practical LES. In addition, the assumption of local equilibrium between the production and dissipation of the kinetic energy (an assumption implicit in all algebraic eddy viscosity models) may be violated. The k-equation model with fixed coefficients was investigated in Menon and Yeung (1994a), while the dynamic k-equation model is investigated in Menon and Yeung (1994b) and Kim et al. (1994).

We are also investigating more advanced models for high Reynolds number flows. One such model is a two-equation model for the subgrid kinetic energy and subgrid helicity (the k-h model). Helicity is non-zero only if the flow is locally 3D. Thus, if the small scales are anisotropic or non-homogeneous (which can occur if the grid is coarse, the geometry is complex, and the Reynolds number is very high) then simple eddy viscosity models or even the one-equation models, may not be able to take into account this small-scale, local 3D effects. Some preliminary studies of this model have been completed and results are discussed below.

### *2.1.1 Summary of the Results*

The results of the analysis of these subgrid models have been reported in the papers attached in the Appendices. Here, we briefly summarize those results and then discuss some new results recently obtained.

The analysis of the eddy viscosity models (models (a) and (c)), the scale similarity model (model (d)) and the one-equation model (model (e)) were reported in Menon and Yeung (1994a). The *a priori* analysis showed that for fine grid resolution, the scale similarity model had the highest cor-

relation with the exact subgrid stresses and energy transfer. However, for a coarse grid LES, this correlation dropped significantly indicating that this model is not appropriate for coarse grid LES. This result was understandable since the scale similarity concept implies that the energy transfer at two grid levels are self similar. As the grid is coarsened, this similarity begins to breakdown. For the low Reynolds number flows studied in Menon and Yeung (1994a), there was no clear inertial range resolved in the DNS. This made it difficult to fully evaluate this model. This model was proposed for high Reynolds number flows (based on experimental data at  $Re=310$ ) where a distinct inertial range existed. Scale-similarity assumptions hold very well in the inertial range and, thus, this model would be applicable. However, this implies that to use this model an inertial range must be resolved in the LES. This may be an unacceptable requirement in high Reynolds number flows (since, it implies a very high grid resolution) and, thus, at present, this model (although very elegant) appears to have limited use for LES of complex, high Reynolds number flows.

Smagorinsky's model (with fixed constant) was quite poor when compared to the other models. The k-equation model (with fixed coefficients) was better than the eddy viscosity model but had a correlation lower than the scale similarity model. Interestingly, when the grid was coarsened, the scale similarity model became poorly correlated; however, the k-equation model did not show such a behavior. This suggests that the k-equation model has the potential for modeling the subgrid stresses and energy transfer in coarse grids.

Subsequent to this *a priori* analysis, these models were implemented in a LES code and simulations were carried out using different grid resolutions. To compare the results, all simulations were begun with nearly identical initial conditions. Thus, at  $t=0$ , all the flow fields were highly correlated. The analysis was carried out at an instant when the flow had evolved to realistic turbulence. The correlation analysis using just the LES data showed a completely different picture. All models showed very poor correlation (compared to *a priori* tests). Both the eddy viscosity model and the scale similarity model appeared to model the subgrid stresses quite poorly compared to the one-equation model.

These results clearly highlight the fact that subgrid models that appear to be quite good in *a priori* analysis may not be as good when implemented in actual LES. Furthermore, it appeared that the k-equation model had the best capability to model the subgrid stresses in coarse grid LES.

The study in Menon and Yeung (1994a), employed the models with fixed coefficients. Since it had been shown by other researchers that the dynamic eddy viscosity model is quite superior to Smagorinsky's classical model, it was decided to revisit these models but by allowing for dynamic evaluation of the coefficients. The dynamic eddy viscosity model and a dynamic version of the k-equation model was then analyzed using the methods developed above. Some of these results will be reported in details in Menon and Yeung (1994b) and Kim et al (1994). It has been shown that the dynamic procedure significantly improves the correlations. An interesting observation was that, compared to the dynamic Germano's model, the dynamic k-equation model showed a much better improvement and was clearly superior for coarse grid LES. This has given confidence that for coarse grid LES for high Reynolds number flows, the use of such higher order models may be beneficial. This is an issue that will be revisited using more complex flows in the second year of this research.

We are now investigating a new two-equation model. The governing equations are shown in the Appendix and the subgrid model is essentially the model proposed by Yoshizawa (1993). We expect that in the course of our study, this model (if useful) will undergo some changes. For example, so far, results have been obtained using fixed coefficients. We expect the dynamic procedure will improve this model and, therefore, we are now in the process of including a dynamic procedure to solve this model.

We simulated a simple periodic flow field for the Taylor-Green Vortex. This field is primarily 2D and will not contain any helicity. This was confirmed by carrying out LES using the k-h model and showing that the subgrid helicity was negligible. Next, the spanwise velocity field was changed by adding a  $\cos x$  term. This allows the large-scales to become 3D while still satisfying continuity. We were interested in determining if this flow field would generate small-scale 3D structures and, if so, would the new k-h model be able to predict the helicity in the unresolved scales.

We looked at three quantities: (1) the correlation between subgrid helicity and large-scale vorticity, (2) the accuracy with which subgrid helicity is being modeled, and (3) the relevance of helicity to the subgrid stresses (that is, the effect of non-eddy viscosity terms in the stress model that appears explicitly due to helicity).

In Fig. 1a and 1b, we show 3D visualization of the vortex tubes (constant vorticity isosurfaces) along with contours of subgrid helicity as predicted by the model. The subgrid helicity is only shown on a certain plane. Figure 1a shows the field as seen in a  $32 \times 32 \times 32$  LES, while in Fig. 1b, the results are shown for a  $16 \times 16 \times 16$  LES. It can be seen that regions of intense vorticity are surrounded by regions of high-magnitude subgrid helicity. This indicates significant production of small-scale helicity by the breakdown of the large scale structures. This result also implies that the unresolved scales may be locally anisotropic.

Correlation between the large-scale helicity (due to the resolved fields) and the subgrid helicity was also computed. This correlation should be very low, in fact, it should ideally be zero, since the model is supposed to compute the subgrid helicity only due to the anisotropy or non-homogeneity in the small-scales and, therefore, should not correlate with the large-scale helicity. The computed correlations were also very small with the  $32 \times 32 \times 32$  LES predicting a value of  $1.03\text{E}-4$  and the  $16 \times 16 \times 16$  LES predicting a value of  $5.6\text{E}-4$ . These results showed that the k-h model has been implemented correctly and appears to be predicting the correct physics.

Correlation between the subgrid helicity modeled in the  $16 \times 16 \times 16$  LES and the subgrid helicity predicted by filtering the  $32 \times 32 \times 32$  LES data into a  $16 \times 16 \times 16$  grid was also carried out. If the model behaves accurately in both grids then this correlation should be high. Our preliminary data showed a correlation of 0.736 which is reasonably high. Figure 2a shows the subgrid helicity computed using the  $32 \times 32 \times 32$  LES data filtered to  $16 \times 16 \times 16$  grid, and Fig. 2b shows the model prediction in the  $16 \times 16 \times 16$  LES. Clearly, the model is behaving reasonable well in both grids.

This study is not yet completed and there are still some unresolved issues. For example, the inclusion of helicity model did not improve the subgrid energy transfer correlation. However, our previous study using fixed coefficients for the k-equation model also showed poor correlation (Menon

and Yeung, 1994a), while with dynamic evaluation, the correlation improved significantly (Kim et al., 1994). Therefore, we are now beginning to evaluate dynamically the constants in this k-h model.

Note that, adding one more equation will increase the computational cost. Therefore, before such models are proposed for LES application, it must be clearly demonstrated that it is superior to the conventional eddy viscosity model. The tests using Taylor-Green vortex or isotropic turbulence may not be appropriate to evaluate this model. Therefore, we are now starting to implement this model into the code developed to simulate more complex flows such as flows past rearward facing steps. If this model is superior for such flows, then the additional cost of computation may be balanced by the ability of the new model to handle complex flows using relatively coarser grids (thereby, decreasing computational cost). This is the primary goal of this research.

## *2.2 Analysis of Compressible Isotropic Turbulence*

Some studies were also carried out to extend the analysis methods to study compressible flows. As noted before, the analysis methods are supposed to be independent of the type of flow field studied and, therefore, with some minor modifications should be applicable in compressible flows. To compare with the incompressible flow results, we began by simulating low Mach number (essentially incompressible) isotropic turbulent flow fields. So far, only the compressible versions of the eddy viscosity model (Erlebacher et al., 1987), the dynamic eddy viscosity model, and the scale similarity model have been implemented and evaluated. Here, we will summarize some of the more recent results of this study. More details of this work will be included in the final version of the paper Menon and Yeung (1994b).

Figures 3a and 3b show, respectively, the correlation of the exact subgrid stress  $\tau_{xx}$  (obtained from  $64^3$  DNS data) with the eddy viscosity model and scale-similarity model predictions as a function of filter width. Again, as before, box filters have been employed. The results for the earlier incompressible data are also shown. These figures show the characteristic decrease in correlation when the grid is coarsened with the scale similarity model showing most rapid decrease. The compressible data is quite close to the incompressible data since very low Mach number flow has been simulated. However, note that, two completely different numerical solvers and subgrid models were employed for this comparison.

Figures 4a and 4b show, respectively, the correlation between exact energy transfer  $\tau_{ij}S_{ij}$  and the modeled energy transfer for the two models. Again, both models show that with decrease in grid resolution, the correlation decreases. The scale similarity model again shows a strong dependence on the grid resolution. However, for relatively fine mesh, the scale similarity model is quite superior to the eddy viscosity model. This is in agreement with the incompressible flow results discussed in Menon and Yeung (1994a).

Since the incompressible study showed that the dynamic subgrid models are superior to the models with fixed coefficients, we are now in the process of evaluating dynamic subgrid models for compressible flows. Preliminary results show good agreement with the results of Moin et al. (1993). More results of this study will be reported in the near future.

### 3. LES OF FLOWS PAST REARWARD FACING STEPS

We are now getting ready to simulate more complex flows such as flows past rearward facing steps. We have completed preliminary validation studies using the simple eddy viscosity model (with no dynamic evaluation) and have demonstrated the ability of our numerical solver to reproduce results consistent with earlier studies. For example, Fig. 5 shows the variation of reattachment distance (normalized by step height) as a function of Reynolds number. Also shown are results obtained by other researchers. Clearly, our LES solver is in good agreement with earlier studies. Figures 6a and 6b show, respectively, the vortical structures downstream of the step for the two Reynolds numbers. As Reynolds number increases, more complex flow patterns are formed as expected.

The above results were obtained using the classical eddy viscosity model. These earlier calculations were carried out to determine the accuracy of the code and to resolve all the programming issues. Therefore, detailed analysis of the data have not been carried out. Since the analysis of subgrid models in isotropic turbulence clearly suggest that the dynamic models are superior, we are now in the process of including the dynamic models into this code. It is expected that all future calculations in this configuration will be carried out using dynamic models (such as the dynamic k-equation and dynamic k-h models) and for relatively high Reynolds numbers. The exact test conditions have not yet been finalized since we want to first make sure that there is sufficient experimental data for model validation in such flows.

### 4. PLANS FOR THE NEXT YEAR

The research carried out in the first year focussed on simple flows such as isotropic turbulence. The methods developed for analysis of subgrid models will now be used for more complex flows. Therefore, from now on, all studies will focus of complex, high Reynolds number flows. Two test flows have been chosen for subgrid model validation studies. The first configuration is the *rearward facing step* described above. The second configuration is a *co-axial jet shear layer with and without swirl*. This type of highly 3D swirling flow occurs in many flow situations and has some interesting features associated with swirl induced mixing. This flow is also sufficiently complex and there is some experimental data for comparison. Both these configurations will be studied using the same numerical solver and subgrid models. We are interested in determining if the same type of subgrid model is capable of simulating accurately these two different types of flows.

### References

Germano, M., Piomelli, U., Moin, P., and Cabot, W. H. (1991) "A Dynamic Subgrid-Scale Eddy Viscosity Model", *Physics of Fluids A*, Vol. 3.

Kim, W.-W., Menon, S., and Chakravarty, V. K. (1994) "A New Dynamic One-Equation Subgrid Model for Large-Eddy Simulations", submitted for presentation at the 33rd AIAA Aerospace Sciences Meeting, January 9-12, Reno, NV.



Menon, S., and Yeung, P.-K. (1994a) "Analysis of Subgrid Models using Direct and Large-Eddy Simulations of Isotropic Turbulence" Paper No. 10, 74th AGARD Fluid Dynamics Panel Symposium on "Application of Direct and Large Eddy Simulation to Transition and Turbulence".

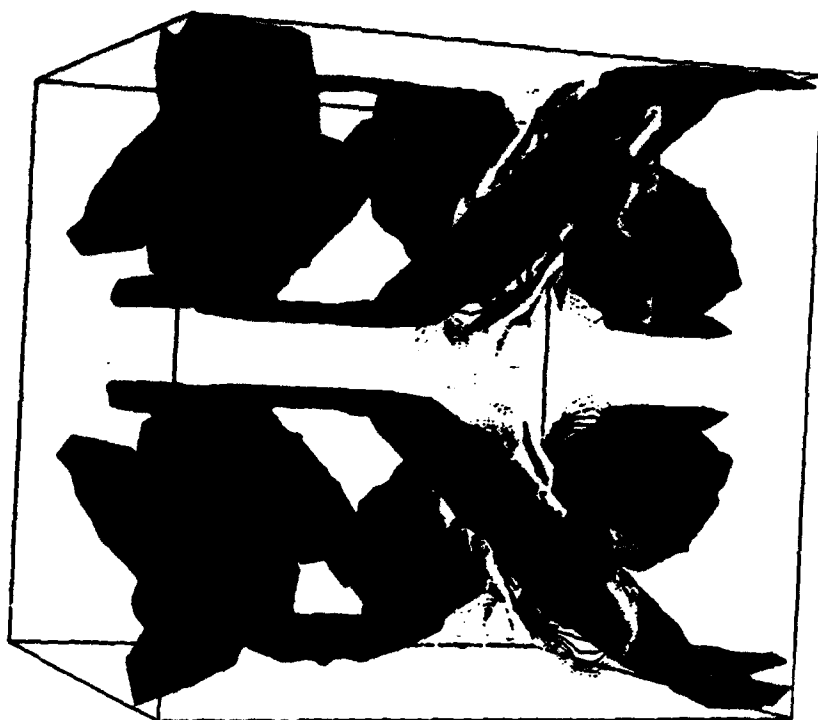
Menon, S., and Yeung, P.-K. (1994b) "Effect of Subgrid Models on the Computed Interscale Energy Transfer in Compressible and Incompressible Isotropic Turbulence" AIAA Paper No. 94-2387, to be presented at the AIAA 25th Fluid Dynamics Conference, June 20-23, 1994, Colorado Springs, CO.

Moin, P., Squires, K., Cabot, W., and Lee, S. (1991) "A Dynamic Subgrid-Scale Model for Compressible Turbulence and Scalar Transport", Physics of Fluids, Vol. 3., pp. 2746-2752.

Yoshizawa, A. (1993) "Bridging between eddy-viscosity type and second-order models using a two-scale DIA" presented at the 9th Symposium on Turbulent Shear Flows, Kyoto, Japan, August 16-18, 1993.

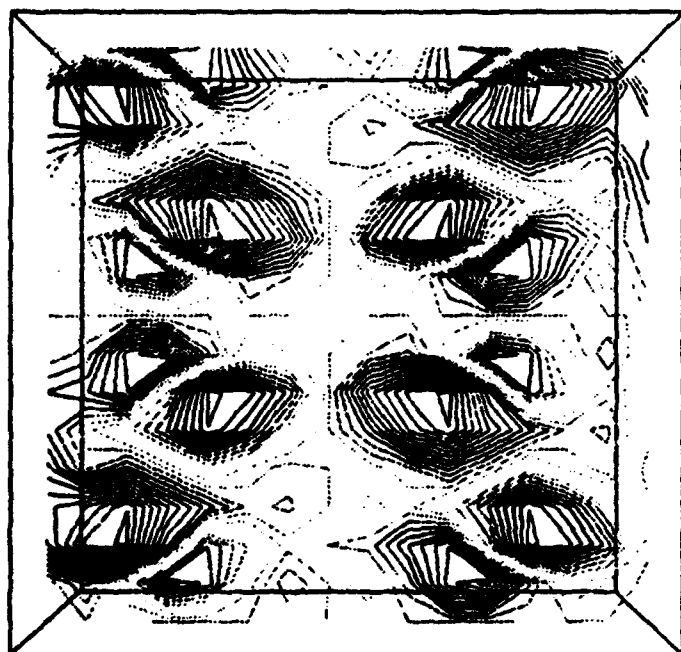


(a) 32x32x32 grid result

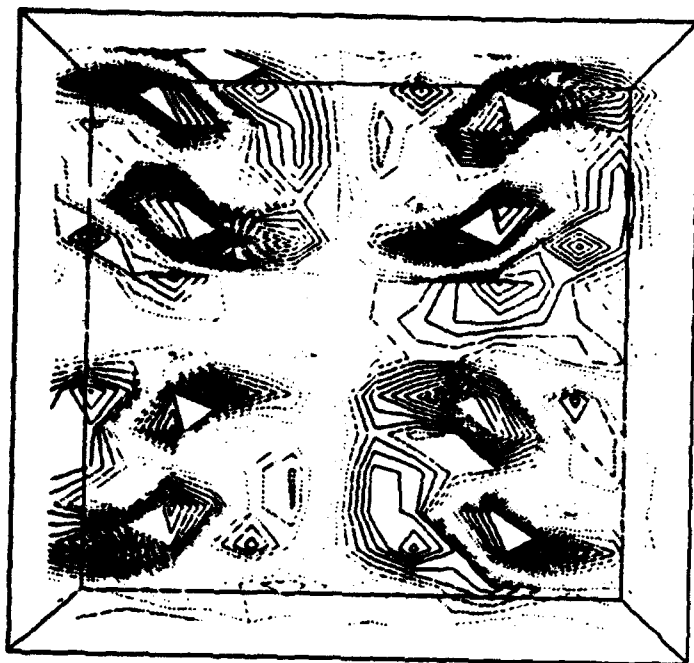


(b) 16x16x16 grid result

Figure 1. Vorticity Isosurfaces and subgrid helicity contours obtained during LES of Taylor-Green vortices.

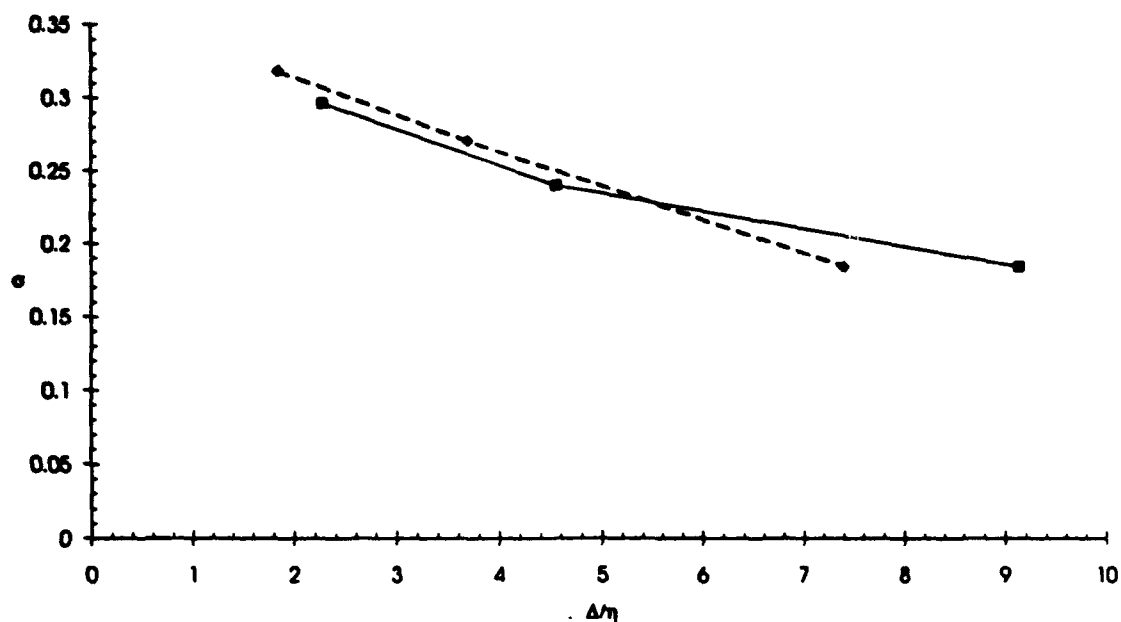


(a) Subgrid helicity in a  $16^3$  grid computed by filtering LES data obtained on a  $32^3$  grid

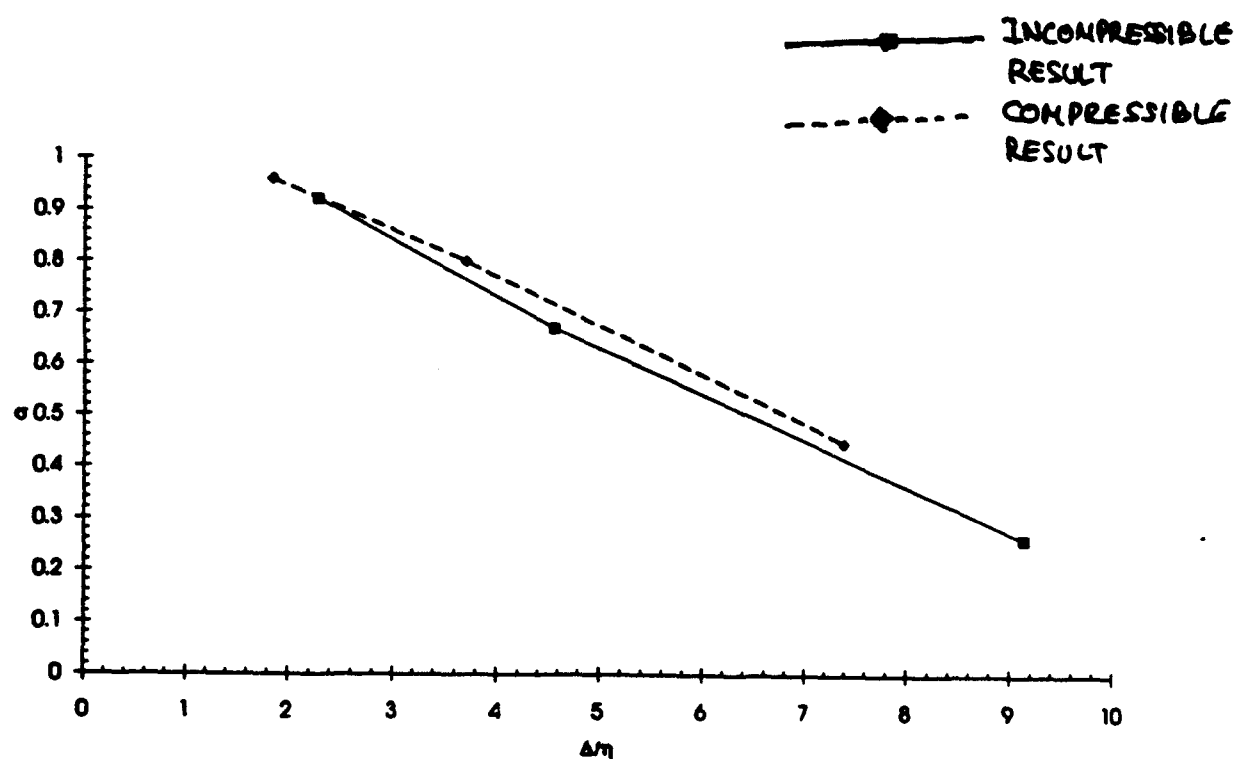


(b) Subgrid helicity obtained during LES on the  $16^3$  grid

Figure 2. Contours of subgrid helicity computed from LES data at an arbitrary x-y plane.



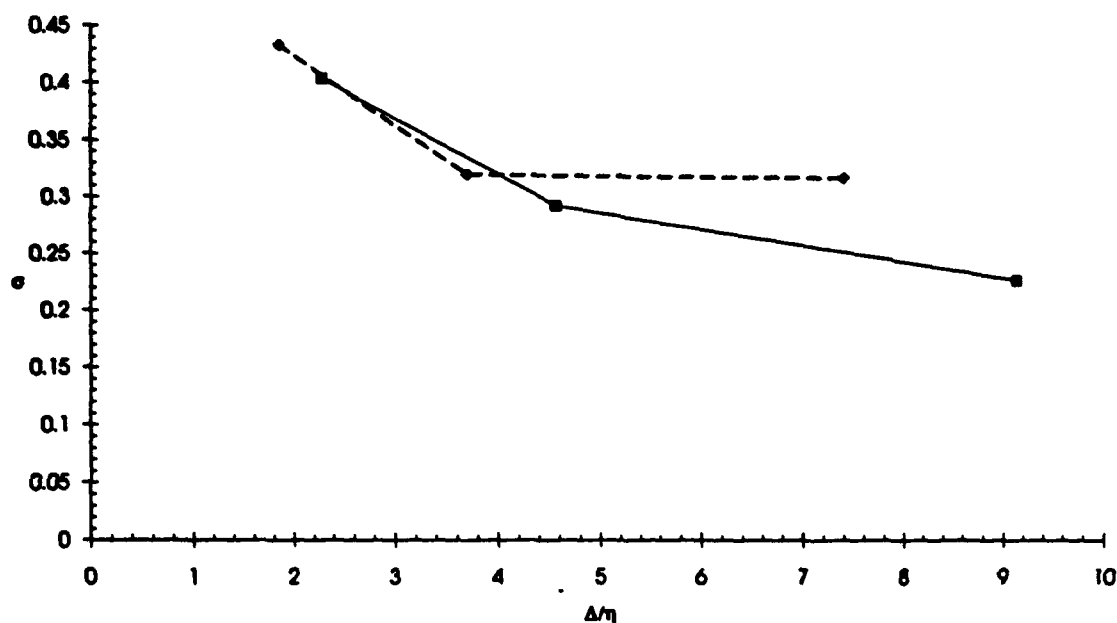
(a) Compressible eddy viscosity model



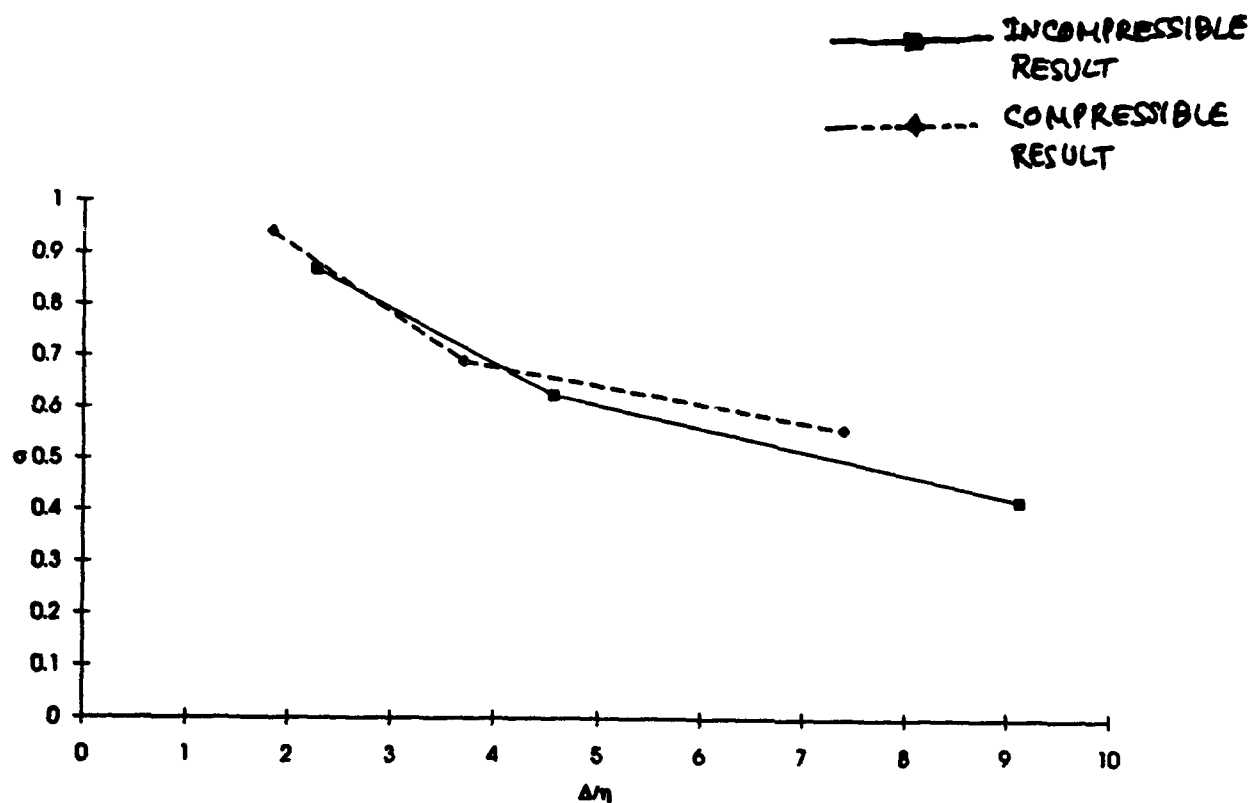
(b) Compressible scale-similarity model

Figure 3. Cross correlation analysis of compressible subgrid models using DNS data of compressible, decaying, homogeneous isotropic turbulence at  $Re = 10$ . Subgrid stress correlation obtained using box filter.

Cor



(a) Compressible eddy viscosity model



(b) Compressible scale-similarity model

Figure 4. Cross correlation analysis of compressible subgrid models using DNS data of compressible, decaying, homogeneous isotropic turbulence at  $Re = 10$ . Subgrid energy transfer correlation obtained using box filter.

Reattachment length normalized by the step height versus Reynolds number.

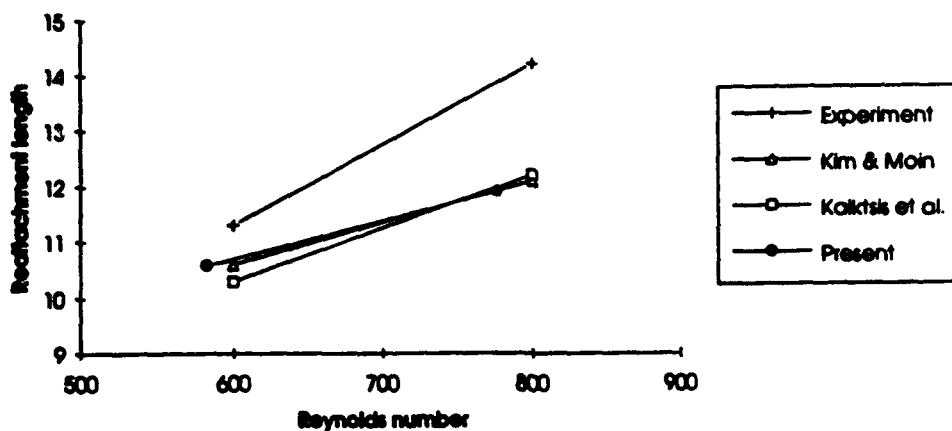
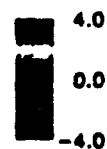


Figure 5. Reattachment length computed from LES of rearward facing step flows for different Reynolds number.

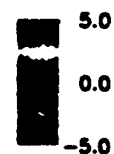
Instantaneous spanwise vorticity contours;  $Re = 777$ .



STEP

(a)  $Re = 777$

Instantaneous spanwise vorticity contours;  $Re = 6992$ .



STEP

(b)  $Re = 6992$

Figure 6. Instantaneous spanwise vorticity contours downstream of the step for different Reynolds number flows

## **APPENDIX I**

## APPENDIX I

### # Two-Equation Subgrid Model for Turbulent Flows

Governing Equations:

$$\frac{\partial \bar{u}_i}{\partial x_i} = 0$$

$$\frac{\partial \bar{u}_i}{\partial t} + \frac{\partial}{\partial x_j} \bar{u}_i \bar{u}_j = - \frac{\partial \bar{p}}{\partial x_i} + \nu \frac{\partial^2 \bar{u}_i}{\partial x_j \partial x_j} + \frac{\partial}{\partial x_i} \tau_{ij}^{sgs}$$

The approach to model the subgrid stresses  $\tau_{ij}^{sgs}$  is to model

- (a) Subgrid kinetic Energy:  $k = \frac{1}{2} (\bar{u}_i'^2 - \bar{u}_i^2)$
- (b) Subgrid Helicity:  $H = (\bar{u}' \cdot \bar{\omega}')$

where  $\bar{u}'$  and  $\bar{\omega}'$  are the subgrid velocity fluctuation and ~~the~~ subgrid vorticity fluctuation

The subgrid model equations are

k-equation

$$\frac{\partial k}{\partial t} + u_i \frac{\partial k}{\partial x_i} = \underbrace{\tau_{ij}^{sgs} \frac{\partial \bar{u}_i}{\partial x_j}}_{\text{Production}} - \underbrace{\epsilon_k}_{\text{Dissipation}} + \underbrace{\frac{\partial}{\partial x_j} \left[ \frac{1}{\sigma_k} (\nu + \nu_T) \frac{\partial k}{\partial x_j} \right]}_{\text{Transport}}$$

H-equation

$$\frac{\partial H}{\partial t} + u_i \frac{\partial H}{\partial x_i} = \underbrace{\tau_{ij}^{sgs} \frac{\partial \omega_i}{\partial x_j} - \omega_i \frac{\partial \tau_{ij}^{sgs}}{\partial x_j}}_{\text{Production}} - \underbrace{\epsilon_H}_{\text{Dissipation}} + \underbrace{\frac{\partial}{\partial x_j} \left[ K \omega_j + \frac{1}{\sigma_H} (\nu + \nu_T) \frac{\partial H}{\partial x_j} \right]}_{\text{Transport}}$$



Here,  $\omega_i$  is the vorticity components of the resolved field, i.e.  $\vec{\omega} = \nabla \times \vec{v}$ .

Also, the model for  $\tau_{ij}^{sgs}$  is represented in terms of both  $k^{sgs}$  and  $H$ :

Thus,

$$\tau_{ij}^{sgs} = -\frac{2}{3} k \delta_{ij} + \nu_T S_{ij} - \eta_H \left[ \omega_i \frac{\partial H}{\partial x_j} + \omega_j \frac{\partial H}{\partial x_i} - \frac{2}{3} \omega_k \frac{\partial H}{\partial x_k} \delta_{ij} \right]$$

Here, the second term in terms of  $H$  is the new term to account for the contribution of anisotropy in the small scale. This term accounts for the non-eddy viscosity contribution and thus, accounts for the deviation from the classical subgrid stress representation.

To close these equations, additional terms have to be defined. These are: (using Yoshizawa's formulation):

$$E = C_E k^{3/2} \Delta, \quad C_E = 0.916, \quad \sigma_k \approx \sigma_H \approx 1.0$$

$$E_H = C_{EH} \frac{E H}{k}, \quad C_{EH} \approx 1.0$$

$$\nu_T = C_\nu k^{1/2} \Delta, \quad C_\nu = 0.0854$$

$$\eta_H = C_\eta \Delta^3 / k^{1/2}, \quad C_\eta \approx 3.86 \times 10^{-3}$$

## **APPENDIX II**

**ANALYSIS OF SUBGRID MODELS USING  
DIRECT AND LARGE EDDY SIMULATIONS  
OF ISOTROPIC TURBULENCE**

**S. Menon and P.-K. Yeung  
School of Aerospace Engineering  
Georgia Institute of Technology  
Atlanta, Georgia 30332-0150**

**Paper No. 10**

**74th AGARD Fluid Dynamics Panel Symposium**

**on**

**"Application of Direct and Large Eddy Simulation  
to Transition and Turbulence"**

**April 18-21 1994**

**Chania, Greece**

# ANALYSIS OF SUBGRID MODELS USING DIRECT AND LARGE-EDDY SIMULATIONS OF ISOTROPIC TURBULENCE

S. Momen and P. K. Young  
School of Aerospace Engineering  
Georgia Institute of Technology  
Atlanta, Georgia, 30332-0150

## ABSTRACT

Direct and large eddy simulations of forced and decaying isotropic turbulence has been performed using a pseudospectral and a finite-difference code. Subgrid models that include a one-equation subgrid kinetic energy model with and without a stochastic backscatter forcing term and a new scale similarity model have been analyzed in both the Fourier space and physical space. The spectral space analysis showed that energy transfer across the cutoff wavenumber  $k_c$  is dominated by local interaction. The correlation between the exact and modeled (by a spectral eddy viscosity) nonlinear terms and the subgrid energy transfer in physical space was found to be quite low. In physical space, a similar correlation analysis was carried out using top hat filtering. Results show that the stress and energy flux predicted by the subgrid models correlate very well with the exact data. The scale similarity model showed very high correlation for reasonable grid resolution. However, with decrease in grid resolution, the scale similarity model became more uncorrelated when compared to the kinetic energy subgrid model. The subgrid models were then used for simulations for a range of Reynolds number. It was determined that the dissipation was modeled poorly and that the correlation with the exact results was quite low for all the models. In general, for coarse grid resolution, the scale similarity model consistently showed very low correlation while the kinetic energy model showed a relatively much higher correlation. These results suggest that to use the scale similarity model relatively fine grid resolution may be required, whereas, the kinetic energy model could be used even in coarse grids.

## 1. INTRODUCTION

For large-eddy simulation (LES) methods to become a viable tool for simulating high Reynolds number flows in complex geometries, models that faithfully represent the effects of the unresolved scales of motion on the resolved motion have to be developed and validated. These unresolved scales act on the resolved field as new unknown stresses that must be modeled (by the so-called subgrid models). The most popular subgrid model is the eddy viscosity model, first proposed by Smagorinsky in 1963. Inherent limitations of this model were identified quite early and methods were developed to address these limitations. Key modifications involved the adjustment of the "constant" (the Smagorinsky constant) for different flows [e.g., 1] and the use of damping functions to model near-wall effects [2].

Although LES using these models have provided fairly acceptable results, recently, more serious limitations have been identified. For example, backscatter of energy from the unresolved to the resolved scales has been observed to occur in direct numerical simulations (DNS) data [3] demonstrating

that the subgrid processes cannot be modeled by a purely dissipative mechanism. Recent attempts to improve the eddy viscosity model involves the dynamic evaluation of the model constant [4] and an explicit modeling of the subgrid backscatter process [5,6]. The dynamic model has proven quite versatile and results show that it can model correctly the behavior of the subgrid stresses both near and away from the wall and has a capability to model backscatter [4,7]. However, it is not yet clear if algebraic subgrid models are adequate for LES of high Reynolds ( $Re$ ) number flows, especially when coarse grid resolutions are employed. This is due to the possibility that the unresolved scales could contain significant amount of turbulent kinetic energy resulting in significant backscatter. Furthermore, anisotropy effects in the unresolved scales may have to be taken into account.

To evaluate subgrid models, *a priori* evaluation of the model(s) using DNS data (obtained in simple, low- $Re$  flows) is typically carried out. Then, the subgrid model is used in a LES using coarse grid resolution and comparisons with DNS predictions are used to determine the validity of the subgrid model. However, models validated using *a priori* analysis of low- $Re$  DNS data appears to have problems when used in high  $Re$  flows. High Reynolds number DNS cannot be carried out and, therefore, *a priori* analysis is no longer possible. The *a priori* methods also have some limitations, since, such analysis is typically carried out in Fourier space which is only possible for flows in configurations that employ periodic boundary conditions. Thus, for high- $Re$  flows in complex domains, new methods to investigate the applicability and validity of the chosen subgrid model have to be developed in physical space. Furthermore, such analysis has to be carried out using only LES. Of course, comparison with experimental data will remain the final test of the model, but if the agreement is poor, methods are needed that will allow the modeler an avenue for improving the subgrid model.

In this paper, the effect of the form of the chosen subgrid model on the energy transfer process between the resolved and unresolved scales in LES, will be investigated. We will address this issue by carrying out DNS and LES of both decaying and forced, incompressible, isotropic turbulence and analyze the data in both physical and spectral space. In the Fourier space, an earlier developed technique [8] was used, while in the physical space methods such as correlation analysis [9] was used. The results of these studies are described below.

## 2. NUMERICAL METHODS

Two simulation methods have been used in this research. The first method is a well known pseudo-spectral method [10] and has been primarily used to obtain high resolution DNS data. No LES has been performed with this code. The second code

is a new finite-difference Navier-Stokes solver that is 5th-order accurate in space and second-order accurate in time. This code has been developed in a very general manner and is used for both LES and DNS. Both simple, (e.g., isotropic turbulence) and relatively complex (e.g., rearward facing steps) flows have been simulated using this code. The numerical algorithm is based on the artificial compressibility method. To obtain time-accuracy at each time step, iterations in pseudo-time is carried out using a multigrid technique until the incompressibility condition has been met. This code has been validated by comparing its predictions to those of the spectral DNS code which are briefly summarized below.

### 2.1. DNS using the Pseudo-Spectral Method

Direct simulations of both (a) naturally decaying isotropic turbulence and, (b) statistically stationary isotropic turbulence in which the turbulent kinetic energy is maintained by stochastic forcing of the large scales [11], have been performed with both  $64^3$  and  $128^3$  grid resolution.

Decaying isotropic turbulence has been simulated by beginning with an isotropic Gaussian random field with a specified initial energy spectrum, and then allowing the hydrodynamic field to evolve until a "realistic" self-similar state has been reached [12]. This developed isotropic state is characterized by Kolmogorov similarity in the high wavenumber energy spectrum, power law decay of energy, and non-Gaussian velocity gradients. DNS data used for analysis in this paper is approximately at a Taylor-scale Reynolds number  $Re_\lambda$  of 20. A higher Reynolds number can be reached by forcing the large scales [11]. The limitation is that the energy transfer characteristics at the large scales are distorted as a result of artificial forcing. However, the structure of the small scales is not directly affected. The parameters of the forcing scheme are chosen to reproduce one realization of the stationary isotropic turbulence studied earlier [12] at a  $Re_\lambda = 90$ .

The energy spectra for both decaying and forced isotropic turbulence, are shown in Figure 1a, with Kolmogorov scaling of the variables. It is clearly seen that the energy in the large scales is greatly increased by the forcing. On the other hand, the spectral shapes at the small scales are very similar. The small spectral turn-ups at the high wavenumber end are caused by imperfect resolution with a finite number of grid points. A nondimensional measure of the numerical resolution is given by  $k_{max}\eta$ , where  $k_{max}$  is the highest wavenumber (90) reached in the simulations, and  $\eta$  is the Kolmogorov length scale. It may be seen from the figure that in both data sets,  $k_{max}\eta$  is about 1.6, which is sufficiently high for adequate resolution of the small-scale motions in the simulations [12].

### 2.2. DNS using Finite-Difference Method

Decaying and forced isotropic turbulence was also simulated using the finite-difference code. The forced simulation employed a forcing method [13] that differed from the stochastic forcing employed for DNS in spectral space. Therefore, direct comparison of the predictions could not be carried out. However, using identical initialization, decaying isotropic turbulence was simulated using both the codes in a  $64^3$  grid resolution. Figure 1b shows the Kolmogorov-scaled energy and dissipation spectra from the spectral and physical space DNS at nearly the same time of evolution ( $t = 12$ ,  $Re_\lambda = 10$ ). Good agreement is obtained in nearly the entire wavenumber space except near the very low wave numbers.

More detailed evaluations of the various statistical quantities (such as the dissipation rate skewness, etc.) showed that the physical space code is capable of reproducing statistics very similar to those obtained by the spectral code.

## 2. SUBGRID ENERGY TRANSFER AND MODELS

Two different methodologies have been employed to analyze the results of the simulations. The first, relies entirely on the Fourier space information and closely follows the method developed earlier by Domaradzki et al. [8]. The second, relies entirely on the physical space information and, at present, employs a variety of techniques to characterize the behavior of the models.

### 2.1. Subgrid Transfer and Modeling in Fourier Space

The Fourier space representation of the Navier-Stokes equations may be written as:

$$\left( \frac{\partial}{\partial t} + \nu k^2 \right) u_k(t) = N_k(t) \quad (1)$$

where  $u_k(t)$  is the velocity field in the Fourier space at a wavenumber mode  $k$  (of magnitude  $k$ ),  $\nu$  is the kinematic viscosity, and  $N_k(t)$  is the nonlinear term which includes the effects of advection, pressure and incompressibility and is given by

$$N_k(t) = -\frac{i}{2} P_{km}(k) \int u_p(t) u_{k-p}(t) dp \quad (2)$$

where  $P_{km}(k) = k_i (\delta_{im} - k_i k_m / k^2) + k_m (\delta_{ik} - k_i k_k / k^2)$ , and  $\delta_{ij}$  is the Kronecker delta tensor. A triad in wavenumber space is a closed triangle formed by the modes  $k$ ,  $p$ , and  $k-p$ . The integral above is taken over all possible triads that may be formed with the mode  $k$  as a member.

Domaradzki et al. [8] introduced a technique in Fourier space which involves a decomposition of the various terms into "resolved" and "subgrid" components. This is accomplished by introducing a wavenumber cutoff at  $k_c$ , and then, for example, the nonlinear term may be decomposed into:

$$N_k(t) = N_k(t|k_c) + N_k^s(t|k_c) \quad (k \leq k_c) \quad (3)$$

The resolved nonlinear term,  $N_k(t|k_c)$ , represents contributions from those triad interactions that couple a resolved mode  $k \leq k_c$  to two other resolved modes (i.e., with both  $p$  and  $k-p$  in the resolved range below  $k_c$ ). On the other hand, the rest of the triad interactions, which couple the resolved modes to subgrid modes (with at least one of  $p$  and  $k-p$  in the subgrid range  $k > k_c$ ), are represented by the subgrid nonlinear term,  $N_k^s(t|k_c)$ .

Energy transfer between different scales is represented by triadic interactions. The total (rate of) energy transfer to a Fourier mode  $k$ , due to its interactions with the subgrid scales, is given by  $T^s(k|k_c) = \text{Re} \left[ u_k^*(t) N_k^s(t|k_c) \right]$ , where the asterisk denotes complex conjugate and  $\text{Re}$  indicates the real part. The subgrid transfer spectrum function is then given by:

$$T^s(k|k_c) = \sum_{k' \in \Delta k} T^s(k'|k_c) \quad (4)$$

Here,  $T^s(k|k_c)$  is a function of wavenumber magnitude  $k$  only, and the shell thickness  $\Delta k$  is taken as unity for convenience. Summation over spectral shells, denoted by  $\sum_{k' \in \Delta k}$

short, is also used in the formation of the energy spectrum function  $E(k)$  from the energy of discrete Fourier modes:  $E(k) = \frac{1}{2} \sum_{\mathbf{n}} u_n(\mathbf{x}) u_n^*(\mathbf{x})$ . The energy spectrum  $E^L(k)$  of the resolved scales (i.e., for  $k \leq k_c$ , signified by superscript  $L$ ) at wavenumber  $k$  evolves by:

$$\frac{\partial}{\partial t} E^L(k) = -2\nu k^2 E^L(k) + T(k|k_c) + T^*(k|k_c) \quad (5)$$

where  $T(k|k_c)$  represents energy transfer from interactions with resolved scales only, and  $T^*(k|k_c)$  represents interactions with subgrid modes which must be modeled in a LES.

A subgrid eddy viscosity is often used to parametrize the subgrid motions, with the spectral subgrid scale (SGS) eddy viscosity defined as [8]:

$$\nu_s(k|k_c) = -\frac{T^*(k|k_c)}{2k^2 E^L(k)}, \quad k \leq k_c \quad (6)$$

The corresponding modeled subgrid nonlinear term is given by:  $N_s^{**}(k|k_c) = -\nu_s(k|k_c) k^2 u_n(k)$ , and the modeled subgrid transfer is  $T^{**}(k|k_c) = \text{Re} \left[ u_n^*(k) N_s^{**}(k|k_c) \right]$ . A straightforward substitution of the definitions presented above leads to the relation:

$$\frac{T^{**}(k|k_c)}{T^*(k|k_c)} = \frac{1}{2} \frac{u_n(k) u_n^*(k)}{E^L(k)}, \quad k \leq k_c \quad (7)$$

A further summation over the spectral shell  $k$  would yield unity on the right hand side, which indicates that the spectral eddy viscosity model accounts for the total energy transfer to a spectral shell correctly. However, it may be seen that this model assumes that energy and energy transfer have the same form of distribution within a given spectral shell. In other words, energy and energy transfer are assumed to be entirely in phase with each other in wavenumber space. This assumption, of course, deviates from the exact spectral equations.

The exact and modeled subgrid nonlinear terms and energy transfers obtained from DNS and LES have been analyzed for a range of  $k_c$ . These results will be discussed in Section 4.

### 3.2. Subgrid Transfer and Modeling in Physical Space

In physical space, the incompressible Navier-Stokes equations are filtered using a spatial filter of characteristic width  $\Delta$  (typically, the grid resolution) resulting in the filtered LES equations:

$$\frac{\partial \bar{u}_i}{\partial t} = 0 \quad (8a)$$

$$\frac{\partial \bar{u}_i}{\partial t} + \bar{u}_j \frac{\partial \bar{u}_i}{\partial x_j} = -\frac{\partial}{\partial x_j} \left[ \frac{\bar{p}}{\rho} \delta_{ij} + \tau_{ij} \right] + \nu \nabla^2 \bar{u}_i \quad (8b)$$

where  $\bar{u}_i(\mathbf{x}, t)$  is the resolved velocity field and the subgrid scale (SGS) stress tensor  $\tau_{ij}$  is defined as:  $\tau_{ij} = \bar{u}_i u_j - \bar{u}_i \bar{u}_j$ . It has been shown that proper choice of the filtering process is essential to maintain model consistency [14]. Various types of filtering processes have been studied in the past, such as the top hat, the Gaussian, and the Fourier cut off filters [9,14]. In the present study, we employ the top hat filter which is considered appropriate for finite-difference methods.

The goal of SGS modeling is to represent the SGS stress  $\tau_{ij}$  in terms of the resolved field  $\bar{u}_i(\mathbf{x}, t)$  in such a manner that the modeled SGS stresses represent as much as possible the exact stresses. In addition, the energy flux to the unresolved scales given by  $E(\Delta) = -\tau_{ij} \bar{S}_{ij}$  must also be modeled reasonably well by the subgrid model. These issues will be addressed in this study.

Various models have been proposed, the most popular one being the Smagorinsky's model:

$$\tau_{ij}^S = -2(C_s \Delta)^2 |\bar{S}| \bar{S}_{ij} \quad (9)$$

where, the superscript  $S$  indicates the model,  $C_s$  is the Smagorinsky's constant and

$$\bar{S}_{ij} = \frac{1}{2} \left( \frac{\partial \bar{u}_i}{\partial x_j} + \frac{\partial \bar{u}_j}{\partial x_i} \right) \quad (10)$$

is the resolved rate-of-strain tensor, where  $|\bar{S}| = 12 \bar{S}_{ij} \bar{S}_{ij}^{1/2}$ . The dynamic modeling approach [4,7] can be used to compute the constant  $C_s$  as a part of the solution, as described elsewhere. At present, we have not implemented the dynamic model in the LES but will consider it in the near future.

Here, we consider two new SGS models for analysis and application. The first is a one-equation model for the subgrid kinetic energy  $k_{sgs} = \frac{1}{2} (\bar{u}_i^2 - \bar{u}_i^2)$ . The motivation behind the choice of this model is two-fold. First, as noted earlier, it is conceivable that in high Reynolds number flows (or when very coarse grids are employed), the unresolved scales may contain energy-containing scales. In this case, the contribution of the subgrid energy to the resolved SGS stresses may have to be explicitly computed. Second, we are also interested in LES of reacting flows. For LES of premixed combustion using a thin flame model, the turbulent flame speed must be determined as a function of the laminar flame speed and the resolved subgrid kinetic energy [15]. In such a case, explicit evaluation of the SGS kinetic energy is required. A compressible version of the  $k_{sgs}$  model is currently being used for LES of premixed combustion in a ramjet [15]. One equation models have been used earlier for channel flows [17,18], and it was shown that it gave more accurate results when very coarse grids were used [18].

The exact equation for  $k_{sgs}$  is first derived by filtering the exact equations for the kinetic energy  $u_i^2/2$  and subtracting from it the exact equation for the resolved kinetic energy  $\bar{u}_i^2/2$ . A possible closure for the terms in the  $k_{sgs}$  equation is considered in the following form:

$$\frac{\partial k_{sgs}}{\partial t} + \bar{u}_j \frac{\partial k_{sgs}}{\partial x_j} = -\tau_{ij}^S \frac{\partial \bar{u}_i}{\partial x_j} - C_1 \frac{k_{sgs}^{3/2}}{\Delta} + \frac{\partial}{\partial x_j} \left[ \frac{\nu_i}{\sigma_s} \frac{\partial k_{sgs}}{\partial x_j} \right]$$

where the three terms on the right-hand-side of Equation (11) represent, respectively, the production, dissipation and transport processes. Here, the subgrid stresses  $\tau_{ij}^S$  (considered equivalent to  $\tau_{ij}$ ) are modeled in terms of the SGS eddy viscosity  $\nu_s$  as:

$$\tau_{ij}^S = -2\nu_s \bar{S}_{ij} + \frac{2}{3} k_{sgs} \delta_{ij} \quad (12)$$

where the SGS eddy viscosity is  $\nu_s = C_2 \sqrt{k_{sgs}} \Delta$ . The model constants are chosen based on earlier study [16] to be  $C_1 = 0.09$ ,  $C_2 = 0.916$  and  $\sigma_s = 1.0$ . It has not yet been est-

blished if these constants or the form of the terms in Eq. 11 are appropriate for high-Re LES. For example, it has been noted using a *a priori* study in channel flow, that the dissipation model in equation (11) is extremely poor [19].

To investigate the behavior of the  $L_{ij}$  model, the terms for the production, dissipation and transport from the exact equation was computed by filtering the DNS data and then correlated with the model terms in Equation (11). The results (not shown) suggests that the transport and production terms in the model equation are correlated quite well with the exact terms (with a correlation greater than 0.6). However, the dissipation term was poorly correlated. This result agrees with the earlier observation that the dissipation model needs to be further improvement. This will be addressed in a future study.

If subgrid scales contain energy-containing eddies, then there is a good chance for backscatter of energy from the subgrid scales to the resolved scales. Furthermore, earlier studies [5,6] have shown that forward scatter (by the eddy viscosity term) and backscatter are two distinct processes. Therefore, these two effects must be modeled separately. Using the results of Chenev [5], a phenomenological model for stochastic backscatter was derived earlier [15] by assuming that the backscatter effect can be modeled by a random force which satisfies certain constraints. The resulting form of the backscatter contribution to the subgrid stress model can be written as:

$$\tau_{ij}^b = C_b \prod \frac{\Delta t^2}{\Delta x} \tilde{u}_i \tilde{u}_j^{1/2} \quad (13)$$

Here,  $C_b$  is a constant of order unity,  $\Delta t$  is the time step of the LES, and  $\prod$  is a random number with zero mean and unit variance. Then, the modeled SGS stresses  $\tau_{ij}^b$  become

$$\tau_{ij}^b = -2\nu_t \tilde{u}_i \tilde{u}_j + \frac{2}{3} k_w \delta_{ij} + \tau_{ij}^b \quad (14)$$

The second model used is a modified scale similarity model proposed by Liu et al. [9]. This model was derived using a *a priori* analysis of high  $Re_\lambda$  ( $= 310$ ) experimental data obtained from a turbulent jet and is of the form:

$$\tau_{ij}^s = c_1 f(l_{12}) L_{ij} \quad (15)$$

where the stress  $L_{ij} = \widetilde{u_i u_j} - \widetilde{u_i} \widetilde{u_j}$  can be computed entirely from the resolved velocity field. Here, the tilde indicates filtering at a scale  $2\Delta$  and is reminiscent of the Germano identity [4]. The constant  $c_1$  was determined in [9] to be around 0.45 at high  $Re_\lambda$ . This model is similar to the scale similarity model proposed earlier [20] and it can be shown that the energy flux to the subgrid scale  $E_L = -L_{ij} \tilde{u}_i \tilde{u}_j$  will exhibit both positive (forward scatter) and negative (backscatter) in the flow. However, it has been noted earlier [9,20], and in the present study, that this backscatter (which may not be real) can result in numerical instability. Hence, to control the backscatter, a scalar function  $f(l_{12})$  is used in terms of  $l_{12}$ , a dimensionless invariant:

$$l_{12} = - \frac{L_{ij} \tilde{u}_i \tilde{u}_j}{\sqrt{L_{ij} L_{ij}} \sqrt{\tilde{u}_i \tilde{u}_i}} \quad (16)$$

Here,  $l_{12}$  represents the alignment between  $L_{ij}$  and  $\tilde{u}_i \tilde{u}_j$  [9]. Various forms of the scalar function  $f(l_{12})$  were proposed in [9] but their validity in LES have not been investigated. Furthermore, the experimental data was a two-dimensional

slice of the flow field and Liu et al. [9] had to make some assumptions to determine the contribution from the third dimension. Therefore, to evaluate this subgrid model, both a *a priori* analysis using DNS results and LES, was carried out. Various forms of backscatter control was studied. However, for LES,  $f(l_{12})$  was chosen following the suggestion by Liu et al. [9] such that  $f(l_{12}) = [1 - \exp(-10/l_{12}^2)]$ , if  $l_{12} \geq 0$ , and  $f(l_{12}) = 0$ , if  $l_{12} < 0$ .

To carry out analysis in physical space, methods that rely entirely on physical space information have been employed. To obtain a measure of the accuracy of the model, correlation coefficient (defined in the usual manner) have been used to quantify the results. These results are discussed below.

## 4. RESULTS AND DISCUSSIONS

In this section, we describe the results of our study using both the DNS and LES using the various models described above. The analysis in the spectral space and physical space are discussed in separate section.

### 4.1. Spectral Space Analysis

Energy transfer information extracted from the DNS data was analyzed to determine the effect of a variable cutoff wavenumber  $k_c$  on energy transfer between the resolved (in an LES sense,  $k \leq k_c$ ) and subgrid ( $k \geq k_c$ ) scale ranges. The SGS eddy viscosity, the subgrid and the resolved energy transfer defined earlier in Section 3.1, are shown in Fig. 2 (a,b,c) for decaying isotropic turbulence (at  $Re_\lambda = 20$ ). It can be seen that the SGS eddy viscosity takes negative, albeit, small values at low  $k/k_c$  for relatively high values of the cutoff wavenumber. This indicates that the SGS energy transfer  $T^*(k|k_c)$  takes on positive values - representing a non-negligible backscatter of energy from the subgrid scales to the resolved scales. The eddy viscosity displays a cup-like behavior at resolved wavenumbers approaching  $k_c$ , consistent with the results of Domaradzki et al. [8] at higher Reynolds number. The formation of these cups may be understood in terms of the local nature of energy transfer in turbulence. An active forward-scending transfer of energy occurring between scales close to  $k_c$  causes a large and negative value of  $T^*(k|k_c)$ , and, hence, a large and positive SGS eddy viscosity. The strength of this local transfer, which is evident in Fig. 2(b), depends, of course, on the energy in scales of size in the order of  $1/k_c$ , and, hence, weakens with increasing  $k_c$ .

In Fig. 2(a) it may be seen that the SGS eddy viscosity at the lowest cutoff wavenumber  $k_c=10.5$  (line A) has a much greater value than the data at higher spectral cutoffs. This is a consequence of the subgrid transfer taking on a more local character as the spectral cutoff is moved to lower wavenumbers. That is, energy transfer between the largest scales and the subgrid scales becomes much more significant if the subgrid range is expanded to include intermediate scales that are closer to the largest scales. The upturn in line A at the low wavenumber end is partly a result of the fall-off in the energy spectrum (see Fig. 1a) as the low wavenumber limit is approached.

The behavior of the resolved energy transfer ( $T(k|k_c)$ ), in Fig. 2(c)), which represents interactions wholly among the resolved scales, is also of interest. The signs of this transfer indicate it is consistently a forward cascade, drawing energy from lower to higher wavenumber modes. At large  $k$ , the resolved interactions close to  $k=k_c$  takes on a nonlocal charac-

ter, and is much weaker than the more local transfer that takes place at lower values of  $k_c$ .

It is of interest to compare the spectral properties of stationary forced turbulence (at  $Re = 90$ ) with turbulence in viscous decay. Because of space limitations, we show only the eddy viscosity for stationary forced turbulence, in Fig. 2(d), although, the resolved and subgrid energy transfer have also been calculated. The comp-like behavior of the SGS eddy viscosity near  $k_c$  is preserved, although, more pronounced than for decaying turbulence. The influence of  $k_c$  on the magnitude of the SGS eddy viscosity and subgrid transfer near  $k_c$  is qualitatively similar to decaying isotropic turbulence. A qualitative difference is observed for  $k_c = 15.5$ , with backscatter and negative eddy viscosity found in the forced turbulence data. For the lowest spectral cutoff  $k_c = 10.5$  (line A), the subgrid viscosity is also much larger than that for higher cutoffs, as in the case of decaying turbulence. On the other hand, no upturn at the low wavenumber end is observed; this can be understood by noting that in the expression for eddy viscosity, the energy spectrum appears in the denominator and in the low wavenumber range, the spectrum is nearly flat (see Fig. 1a).

Since the lowest wavenumber modes are forced in stationary turbulence, the resolved energy transfer is greatly distorted. In this forced turbulent flow, the peak in the energy spectrum occurs at the lowest nonzero wavenumber shell in the simulation. While the nature of a forward cascade remains unchanged, these forced modes, being highly energetic, lose a large amount of energy to other resolved modes (and, for low spectral cutoffs, to the subgrid scales as well).

To assess the performance of the SGS eddy viscosity model (Eq. 6), an important criterion is how well the energy transfer is predicted in physical space. The Fourier space considerations illustrated by Eq. 8 indicate, in homogeneous turbulence, the space average of the energy transfer is reproduced exactly by this model. However, incorrect phase information in Fourier space translates to deviations from exact values at each grid point in physical space. A quantitative measure of model accuracy is the correlation coefficient between the exact and modeled SGS transfer in physical space, denoted by  $T^*(x|k_c)$  and  $T^m(x|k_c)$ , respectively. This correlation coefficient,  $\rho(T^*, T^m)$ , which is computed over all grid points in physical space, is shown in Fig. 3 as a function of the cutoff wavenumber  $k_c$ . Also shown, is the corresponding correlation coefficient, averaged over the coordinate components, between the exact and modeled SGS nonlinear terms, denoted by  $\rho(N^*, N^m)$ .

Several observations may be made in Fig. 4. First, for all of the quantities considered, model performance improves steadily with increasing cutoff wavenumber. This is clearly consistent with the general expectation that SGS models should improve if a wider range of scales are resolved in an LES by increasing the number of grid points, leaving only the smallest scales to be modeled. Second, except at low cutoff wavenumbers, the nonlinear term is predicted more accurately than the energy transfer. Since in physical space this (subgrid) transfer is given by the dot product between the resolved velocity vector and the subgrid nonlinear vector, we may conclude that the alignment between these vectors is not well predicted. Third, the model produces better agreement with DNS data in the decaying case compared to the forced case. This is not surprising, since the artificial forcing has a

distorting effect on energy transfer, especially at the large scales, which generally dominate the correlation coefficients.

As discussed above, one of the weaknesses of the SGS spectral eddy viscosity model is that it is based on quantities summed over spectral shells. As a result,  $\nu_t$  is represented as an isotropic function of the wavenumber magnitude  $k$  in Fourier space. A modification can be made to accommodate the phase variations inside spectral shells by using the modal transfer and energy instead. We define the modified SGS spectral eddy viscosity by

$$\nu_t(k|k_c) = -\frac{T^*(k|k_c)}{k^3 u_r(k)u_r(k)} \quad k \leq k_c \quad (17)$$

The modeled SGS nonlinear term becomes  $Re(u_r^*(k)N_c^*(k|k_c)/u_r^*(k))$ , which is, clearly, still not exact. This modified model requires too much information - the energy and SGS transfer at individual Fourier modes - to be useful in practice. However, because it accounts for phase variations within spectral shells, this modified model does give better agreement with DNS data. The correlation coefficients in physical space discussed above, but computed from the modified model, are shown as lines E and F in Figure 4 for the decaying turbulence case. As may be seen, these correlation coefficients are consistently higher than those obtained from the conventional model.

The spectral space analysis method was then used to analyze the behavior of the subgrid models described in Section 3.2. Figure 4a shows the Kolmogorov scaled energy spectra for the  $64^3$  DNS (at a  $Re = 10$ ), and for  $32^3$  and  $16^3$  LES using the  $k_{eq}$  model with stochastic backscatter (Equation 14), and the scale-similarity model (Equation 15) at around time,  $t = 12$  which corresponds to around 21.7 large-eddy turnover time. The LES simulations were performed by first filtering the  $64^3$  initial field (i.e., at  $t = 0$ ) in physical space into the LES grid using the top hat filter. Thus, at  $t = 0$ , all the initial fields were highly correlated in the physical space. (Results of the physical space analysis will be discussed in the next section). However, in Fourier space, due to the form of the transfer function for the top hat filter, the initial energy spectra will be quite different for the direct and large eddy simulations. This would show up in the eventual evolution of the flow field when analyzed in the Fourier space. However, if the simulations are self consistent, the Kolmogorov scaled spectra should exhibit similarity, as seen in Figure 4a.

Figure 4b and 4c show, respectively, the energy spectra (normalized by the kinetic energy) and dissipation spectra (normalized by the dissipation rate) as a function of wavenumber. The disagreement between the DNS and LES results is more apparent in these figures. The normalized energy spectra shows that all the LES data predict higher peak energy at a lower wavenumber than predicted by DNS. Both the  $k_{eq}$  and similarity models predict nearly the same peak value (about 25 percent higher than exact) and location with  $32^3$  resolution. However, as the grid is coarsened, the  $k_{eq}$  model shows a much larger peak energy than the similarity model. Further, near  $k = k_{min}$ , the energy in the high wavenumbers is much lower for the LES. The dissipation spectra peaks at larger wavenumbers (by a factor of 2) and all the data shows similar trends. However, since energy is lower near  $k = k_{min}$ , the LES results predict lower dissipation when compared to the DNS results. These results suggest that the dissipation modeled by the subgrid models is insufficient and needs to be improved.



The energy transfer in the spectral space was also analyzed using these LES data. Using the DNS and LES fields shown in Figure 4, the spectral eddy viscosity and the subgrid transfer at a cutoff wavenumber  $k_c = 10$  was computed and are shown in Figures 5a and 5b, respectively. Note that, for the DNS,  $k_{max} = 30$ , while for the LES,  $k_{max} = 15$ . Therefore, a  $k_c$  of 10 is in the range of resolved scales for all the simulations. Figure 5a shows that the spectral eddy viscosity behavior in all cases is nearly identical suggesting that the LES models are behaving quite well. However, this is somewhat misleading. Figure 5b shows that at  $k/k_c \rightarrow 1$  both the scale similarity model and the  $k_{sgs}$  model predict lower negative values for the subgrid transfer  $T^*(k|k_c)$ . A low value for the transfer would result in a lower peak in the eddy viscosity. However, less energy is being transferred to the subgrid scales, as seen in Figure 4. Therefore, the combination of low (negative) value of  $T^*(k|k_c)$  and lower  $E^L(k)$  near  $k_c$  results in an eddy viscosity (from Eq. 6) that appears to agree with the *a priori* results.

In summary, the *a priori* analysis of the DNS data showed that the eddy viscosity model in spectral space has a distinct drop at the wavenumber cutoff  $k_c$ , suggesting that the energy transfer across  $k_c$  is dominated by interaction of scales (both resolved and unresolved) in the neighborhood of  $k_c$ . The spectral subgrid transfer was found to be quite dependent on  $k_c$  and inverse transfer (backscatter) was found to occur for relatively high values of  $k_c$ . Correlation analysis of the nonlinear terms and SGS transfer in physical space showed very low values (around 0.3-0.4) which increased with  $k_c$ . The correlation of the nonlinear term was higher than for the energy transfer indicating that the resolved velocity field and the nonlinear term were not correlated very well.

The analysis of the LES data using a similar method showed that there were significant differences in the energy and dissipation spectra for all the cases studied. This is understandable since the initial spectra for the LES were different from that for the DNS as a result of initialization that maintained high correlation in the physical space. All the SGS models appear to model dissipation very poorly and, also, predict much higher energy in lower wavenumbers than predicted by the DNS data. Using a spectral cutoff at  $k_c = 10$ , it was shown that the spectral eddy viscosity computed using the LES data agrees reasonably well with the eddy viscosity computed using DNS data. However, it was shown that this agreement was due to a combination of lower energy at  $k_c$ , and a lower (negative) value for the subgrid transfer.

## 4.2. Physical Space Analysis

The analysis in the physical space was carried out using methods that attempted to quantify the behavior of the models in terms of the resolution of the large-scale structures and, the correlation between the exact and the modeled stresses and energy flux to the subgrid scales. The *a priori* analysis was carried out on all the DNS data sets. Here, we will discuss representative results.

Figure 6a shows contours of the energy flux ( $E(\Delta) = -\tau_y \bar{u}_y$ ) to the subgrid scales on a  $32^3$  grid obtained by filtering of the  $128^3$  DNS data forced stationary turbulence. This result is compared to the prediction by the  $k_{sgs}$  model without backscatter (Figure 6b), and the scale similarity model without backscatter control (Figure 6c), and with backscatter control (Figure 6d). The contour interval is the same for all figures, and an arbitrary (but same) slice of the 3D field is shown.

Comparison with the exact results (Figure 6a) shows that there is significant similarity in regions with high positive transfer. However, only the similarity model without backscatter control (Figure 6c) is capable of resolving regions with backscatter, although, the peak negative value is over 35 percent lower than in the exact case. The peak positive value is, also, not predicted very well, with the  $k_{sgs}$  model predicting a maximum level that is nearly 60 % lower than the exact value while the similarity model predicting peak level around 35 % lower without backscatter control. With backscatter control, the similarity model predicts a peak level around 42 % lower.

To further quantify the differences and similarity between the model predictions and the exact values, Figure 7a shows the correlation between the exact and the modeled stresses for the forced  $128^3$  DNS data. The correlation shown in Figure 7a is an average of the correlation coefficient of the three stress components ( $\tau_{xx}$ ,  $\tau_{yy}$ ,  $\tau_{zz}$ ). The data shows that the correlation decreases with an increase in filter width for all cases, with the similarity model showing the largest decrease. The similarity model with backscatter control has lower correlation when compared to the same model without backscatter control. This is consistent with the results shown by Liu et al. [9]. The eddy viscosity model of Smagorinsky consistently shows the lowest correlation, as seen in earlier studies. The  $k_{sgs}$  model shows quite high correlation for these stresses with only a weak dependence on the filter width. The correlation for the stresses  $\tau_{ij}$ ,  $i \neq j$  (not shown) was lower than the correlation shown here; however, they too showed only a weak dependence on the filter width. This suggests that as the grid resolution becomes coarser, the  $k_{sgs}$  model should behave much better than the other models shown in Figure 7a.

Figure 7b shows the stress correlation for the subgrid models for two different Reynolds number. The  $k_{sgs}$  model consistently shows higher correlation than the similarity model (with backscatter control) which shows a decrease in the correlation with decrease in  $Re_\lambda$ . The decrease in the stress correlation for the similarity model with increase in filter width and with decrease in  $Re_\lambda$  can be understood by noting that this model was developed based on analysis of very high  $Re_\lambda$  experimental data with at least a decade of wavenumbers in the inertial range. For the present DNS data, there is no appreciable inertial range and this situation is even worse for the low  $Re_\lambda$  case. Furthermore, the model assumes that there is similarity between the stresses resolved at  $2\Delta$  grid and the stresses resolved at the  $\Delta$  grid. In the present case, as the filter width increases (or as the grid coarsens), this assumption breaks down.

Figure 8a shows the energy flux correlation for  $Re_\lambda$  of 90 for the models shown in Figure 7 and Figure 8b shows the energy flux correlation for the models for two different Reynolds numbers. As noted earlier, the energy flux to the unresolved scales is defined as  $E(\Delta) = -\tau_y \bar{u}_y$  at a filter width  $\Delta$  for the exact energy flux. For the subgrid models,  $\tau_y$  is replaced by the appropriate model (e.g., Equations 12 and 15). For small values of  $\Delta/\eta$ , where  $\eta$  is the Kolmogorov scale, the correlation for the scale similarity model is much higher than for the other models. In all cases, the correlation decreases with decrease in Reynolds number with the largest decrease seen for the similarity model.

Since the ensemble-averaged value of the energy flux  $\langle E(\Delta) \rangle$  should be of the order of the dissipation rate  $\epsilon$ , a comparison was carried out for all the models studied here. The results

(not shown) indicates that all models predicted values lower than the dissipation rate computed from the exact field. However, the predicted  $\langle \epsilon(\Delta) \rangle$  was of the same order as the dissipation rate. This agreed with the observations by Liu et al. [9]. The energy flux at scales larger than  $\Delta$  is also of interest. For example, it was shown [9] that the energy flux at a scale  $2\Delta$  can be represented by contributions from the 'local' and 'not-so-local' contributions. Using the Germano identity, the energy flux at  $2\Delta$  can be written as:  $E(2\Delta) = -(L_{ij}\bar{u}_j + \tau_{ij}\bar{u}_j)$ , where as before, the slide filter indicates filtering at the  $2\Delta$  scale. The first term represents the 'local' transfer of energy flux from large scales to scales between  $\Delta$  and  $2\Delta$ , while the second term represents the energy transfer to the scales smaller than  $\Delta$  [9]. A correlation between these two terms was computed for various filter width. The results (again, not shown for brevity) indicates a very high correlation in the range of 0.8, and since  $E(2\Delta)$  was always positive, this suggests that both the energy fluxes were forward scattered. A similar high correlation and behavior was noted by Liu et al. [9] in their *a priori* analysis of the experimental data.

The coefficient  $c_1$  in Eq. 15 was determined by Liu et al. [9] by assuming that the correct amount of dissipation must be predicted by the model. Thus,  $c_1 = \langle \tau_{ij}\bar{u}_j \rangle / \langle f(u_{ij}) L_{ij}\bar{u}_j \rangle$  where  $\langle \rangle$  denotes ensemble averaging. A value of around 0.45±0.15 was estimated for the high Reynolds number experimental data [9]. For the correlation analysis shown in Figures 7 and 8,  $c_1 = 0.45$  was employed. However, in the present study a significant variation in the correlation was observed as a function of both the filter width and  $Re_\lambda$ . Therefore, this coefficient was recomputed using the above noted relation. Figure 9 shows the variation of  $c_1$  as a function of filter width and  $Re_\lambda$ . The results suggest that this coefficient increases with increase in filter width and decrease in  $Re_\lambda$ . However, for small filter widths, the predicted value is in the range of the values determined by Liu et al. [9] from the high  $Re_\lambda$  data. The large variation in the value of  $c_1$  may be an artifact of the limited range of scales resolved in the present DNS data and the problems with the similarity model (discussed above) when the grid is coarsened. This issue needs further study.

*A priori* analysis of the DNS data at  $Re_\lambda = 10$  was also carried out since this data is used for comparison with LES predictions (as discussed in Figure 4). Comparison of the flow structures, and, the stress and energy flux correlations showed a picture very similar to that seen at the higher  $Re_\lambda$  (and therefore, not shown). The scale similarity model consistently showed a much better correlation for both stresses and the energy flux when compared to the  $k_{eq}$  model while the Smagorinsky's model consistently gave very low correlation. In all cases, the correlation decreased with increase in the filter width.

The subgrid models were then implemented in LES using  $32^3$  and  $16^3$  grid resolutions. For LES, the flow field was initialized by a field that was the filtered initial field used for the  $64^3$  DNS. Hence, at  $t=0$  the physical space fields were highly correlated (although, in the Fourier space there was quite a bit of discrepancy, see Figure 4). However, the results showed that as time evolved, the DNS and LES became highly uncorrelated. This can easily be determined by visualizing the flow structures in the DNS and LES fields. This points to the fact that results from *a priori* analysis do not provide the proper guidelines for evaluating the behavior of the

subgrid models in an actual LES.

This was further confirmed by carrying out the correlation analysis. To analyze the LES results, the DNS data obtained on the  $64^3$  grid resolution, and the LES data obtained on the  $32^3$  grid were filtered to the  $16^3$  grid. Then, the energy flux predicted from these two simulations at the  $16^3$  grid resolution was compared to the model prediction in the actual  $16^3$  grid LES. The results showed that all the models predicted very poor correlation (less than 0.1) when the  $16^3$  grid LES was compared to the filtered DNS data set at the same grid level. The comparison between the two LES showed that the energy flux correlation for the scale similarity model was very low (around 0.12) while the  $k_{eq}$  model predicted a relatively higher value of around 0.35. This again suggests that when coarse grids are employed in LES, the  $k_{eq}$  model appears to behave much better. At this juncture, however, the scale similarity model cannot be disregarded since, as noted above, even the *a priori* estimates showed that, in coarse grids the scale similarity assumptions may be breaking down. It is, therefore, necessary to revisit this analysis using LES at much higher  $Re_\lambda$  with a reasonable resolution of the inertial range. This has not been attempted since it requires excessive grid resolution and computational resources.

Instead, a series of simulations were carried out using the  $32^3$  and  $16^3$  grid resolution for an initial  $Re_\lambda = 10^3$ . This is a very high Reynolds number and is probably beyond the capability of the subgrid models used in this study. Therefore, the results of this study can only be qualitatively analyzed by carrying out relative comparison of the behavior of the subgrid models. However, note that, in high Reynolds number flows, the grid resolution that is economically practical is likely to be too coarse to resolve the inertial range.

Figure 10 shows the energy spectra for these high Reynolds number simulations at a time of  $t = 12$ . It was found that the scale similarity model did not contain sufficient dissipation and therefore, for these simulations, the Equation 15 (with  $f(u_{ij}) = 1$ ) was supplemented by a Smagorinsky's eddy viscosity model, in effect, making this model a modified version of the mixed model proposed earlier [20]. The spectra shows that both the modified similarity model and the  $k_{eq}$  model behaves in a similar manner. The spectra for all cases appears to be leveling off at around the same location and it is clear that the cutoff occurs at a wavenumber at which significant energy containing scales remain unresolved. This is as expected for such high Reynolds number simulations.

The stress and energy flux correlation between the  $32^3$  grid and the  $16^3$  grid LES was carried out for this case. Figures 11a and 11b show, respectively, the stress and energy flux correlations (obtained in the  $16^3$  grid) as a function of the initial  $Re_\lambda$ . As discussed before, the computed correlation in the LES is much lower than in the *a priori* analysis. Furthermore, with increase in  $Re_\lambda$ , the correlation for all the models decrease indicating a serious problem with the dissipation modeling. The  $k_{eq}$  model without the stochastic backscatter model (Equation 13) showed a slightly lower correlation indicating that the backscatter model (although not very effective) does result in a higher correlation. More importantly, for all the cases studied here, the  $k_{eq}$  model showed a much higher correlation at this grid resolution. This suggests that although the  $k_{eq}$  model needs improvements, it warrants further investigation for application in high Reynolds number flows.

## 8. CONCLUSIONS

Direct and large eddy simulations of forced and decaying isotropic turbulence has been performed using a pseudospectral and a finite-difference code. Subgrid models that include a one-equation subgrid kinetic energy model with and without a stochastic backscatter forcing term and a new scale similarity model have been analyzed in both the Fourier space and physical space using high resolution DNS data. The spectral space analysis showed that energy transfer across the cutoff wavenumber  $k_c$  is dominated by local interaction. Correlation analysis of the modeled and exact nonlinear terms and the subgrid energy transfer in physical space showed very low values.

In physical space, *a priori* analysis of the stress and energy transfer correlation between the exact values and the modeled terms was carried out for a range of  $Re_\lambda$ . Results show that the stress and energy flux predicted by the both the subgrid models correlates very well with the DNS data with the scale similarity model showing very high correlation for reasonable grid resolution. However, with decrease in grid resolution, the scale similarity model becomes more uncorrelated when compared to the kinetic energy model.

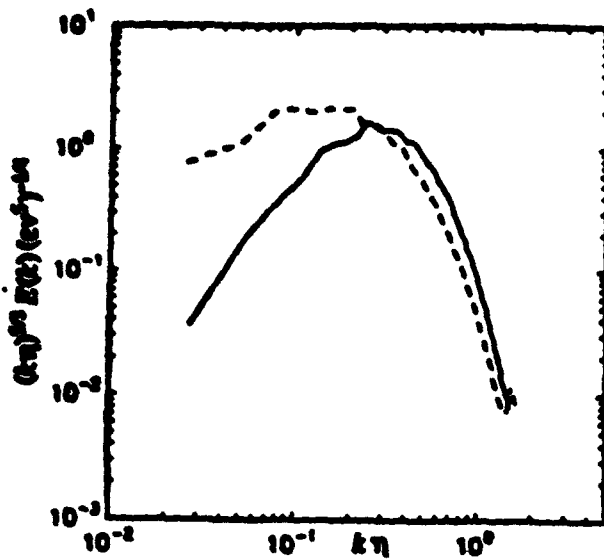
When the subgrid models were used for LES, correlation with the DNS results was very low. This was in spite of keeping the initial flow field for all the simulations highly correlated. This suggests that the results of *a priori* analysis cannot be used to predict the behavior of the subgrid models in actual LES. The analysis of the LES data obtained on very coarse grids showed that the scale similarity model behaves very poorly when compared to the  $k_{eq}$  model which consistently showed much higher correlation. These results suggest that the scale similarity model can be used only for relatively fine grid resolution, whereas, the kinetic energy model can be used even in coarse grids. This was further demonstrated by carrying out LES at a very high  $Re_\lambda$  for which the scale similarity model had nearly zero correlation while the  $k_{eq}$  model still had (albeit) finite value.

## ACKNOWLEDGEMENTS

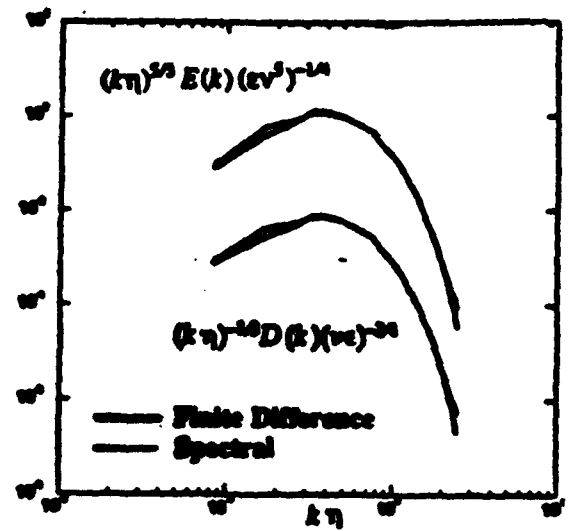
This work is supported by the Office of Naval Research under Grant No. N00014-93-1-0342. Computing time was provided by the Numerical Aerodynamic Simulation (NAS) at NASA Ames Research Center and is gratefully acknowledged. Support provided by graduate students W. Kim and K. Chakravarthy is also acknowledged.

## REFERENCES

- McMillen, O.J., Ferziger, J.H., and Rogallo, R.S. "Tests of new Subgrid-Scale Models in Stirred Turbulence" AIAA Paper No. 80-1339, 1980.
- Moin, P. and Kim, J., "Numerical Investigation of Turbulent Channel Flow", *J. Fluid Mech.*, **118**, pp. 341-377, 1982.
- Piomelli, U., Cabot, W.H., Moin, P., and Lee, S. "Subgrid-scale Backscatter in Turbulent and Transitional Flows", *Phys. Fluids A*, **3**, pp. 1766-1771, 1991.
- Gomano, M., Piomelli, U., Moin, P., and Cabot, W. H. "A Dynamic Subgrid-Scale Eddy Viscosity Model", *Phys. Fluids A*, **3**, pp. 1760-1765, 1991. S. Chasnov, J. R. "Simulation of the Kolmogorov Inertial Subrange Using an Improved Subgrid Model", *Phys. Fluids A*, **3**, pp. 188-220, 1991.
- Leith, C.E., "Stochastic Backscatter in a Subgrid-scale Model: Plane Shear Mixing Layer", *Phys. Fluids A*, **2**, pp. 297-299, 1990.
- Piomelli, U., "High Reynolds Number Calculations using the Dynamic Subgrid-Scale Stress Model", *Phys. Fluids A*, **5**, pp. 1484-1490, 1993.
- Domaradzki, J. A., Liu, W., and Brachet, M. E. "An Analysis of Subgrid Scale Interactions in Numerically Simulated Isotropic Turbulence", *Phys. Fluids A*, **5**, pp. 1747, 1993.
- Liu, S., Meneveau, C., and Katz, J. "On the Properties of Similarity Subgrid-scale Models as Deduced from Measurements in a Turbulent Jet", preprint, submitted for publication, 1993.
- Rogallo, R. S. "Numerical Experiments in Homogeneous Turbulence," NASA TM 81315, 1981.
- Eswaran, V. and Pope, S.B. "An Examination of Forcing in Direct Numerical Simulations of Turbulence", *Comput. & Fluids*, **16**, pp. 257-278, 1988.
- Yeung, P. K. and Brasseur, J. G., "The Response of Isotropic Turbulence to Isotropic and Anisotropic Forcing at the Large Scales," *Phys. Fluids A*, **3**, pp. 884-896, 1991.
- Kerr, R.M., "Velocity, Scalar and Transfer Spectra in Numerical Turbulence" *J. Fluid Mech.*, **211**, pp. 309-332, 1990.
- Piomelli, U., Moin, P., and Ferziger, J.H., "Model Consistency in Large Eddy Simulation of Turbulent Channel Flows", *Phys. Fluids*, **37**, pp. 1884-1891, 1988.
- Memon, S. "A Numerical Study of Secondary Fuel Injection Control of Combustion Instability in a Ramjet", AIAA Paper No. 92-0777, 1992.
- Yoshizawa, A. "Bridging between Eddy-viscosity-type and Second-order Models using a Two-Scale DIA", Ninth Symposium on "Turbulent Shear Flows", Kyoto, Japan, August, 1993.
- Schumann, U., "Subgrid Scale Model for Finite Difference Simulation of Turbulent Flows in Plane Channels and Annuli", *J. Comput. Phys.*, **18**, pp. 376-404, 1975.
- Horiuti, K., and Yoshizawa, A., "Large Eddy Simulation of Turbulent Channel Flow by 1-Equation Model", in *Finite Approximations in Fluid Mechanics*, ed. E. H. Hirschel, pp. 119-134, 1985.
- Piomelli, U. "Applications of Large Eddy Simulations in Engineering: An Overview", in "Large eddy Simulations of Complex Engineering and Geophysical Flows", B. Galperin and S. Orszag, Eds., Cambridge University Press, 1993, pp. 119-137.
- Badrina, J., Ferziger, J.H., and Reynolds, W.C., "Improved Subgrid Scale Models for Large Eddy Simulations", AIAA Paper 90-1357, 1980.



(a) Energy spectra for 128<sup>3</sup> DNS of forced stationary isotropic turbulence at  $Re_\eta = 90$  (dashed line) and decaying turbulence at  $Re_\eta = 20$  (solid line).



(b) Energy and dissipation spectra for 64<sup>3</sup> DNS.

Figure 1. Kolmogorov scaled energy and dissipation spectra for decaying and forced isotropic turbulence.

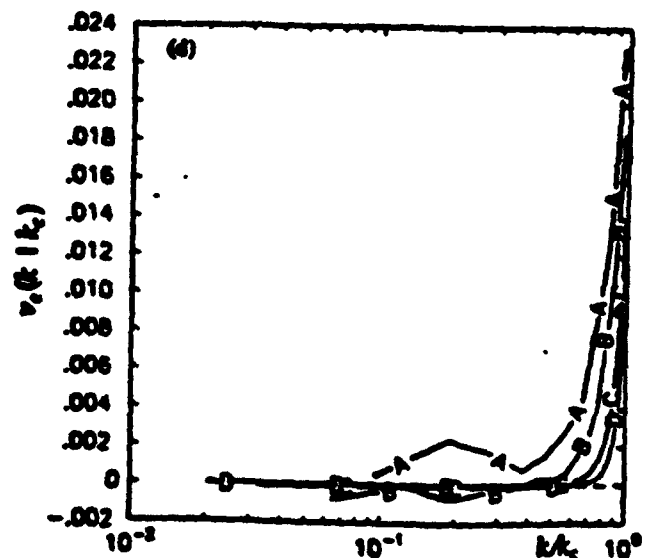
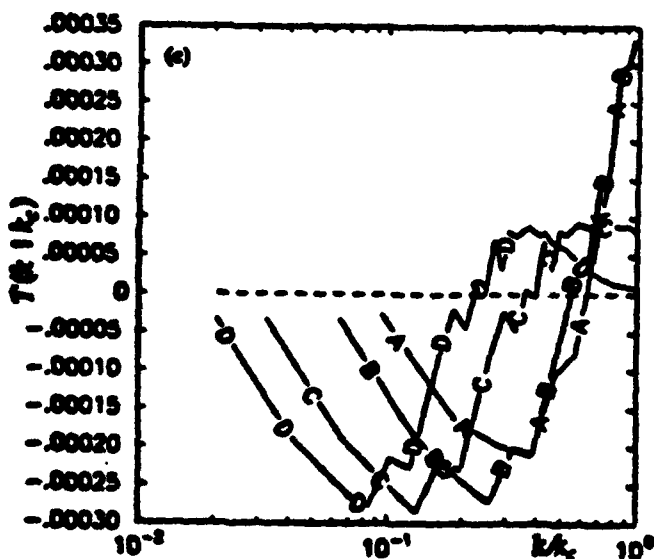
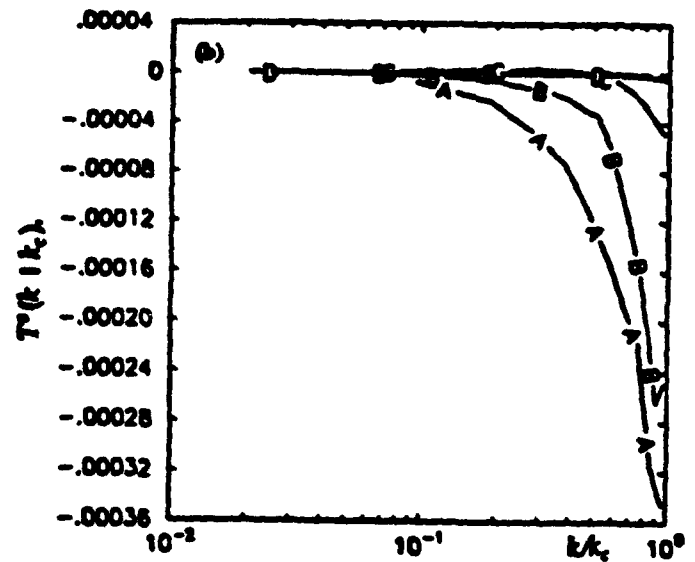
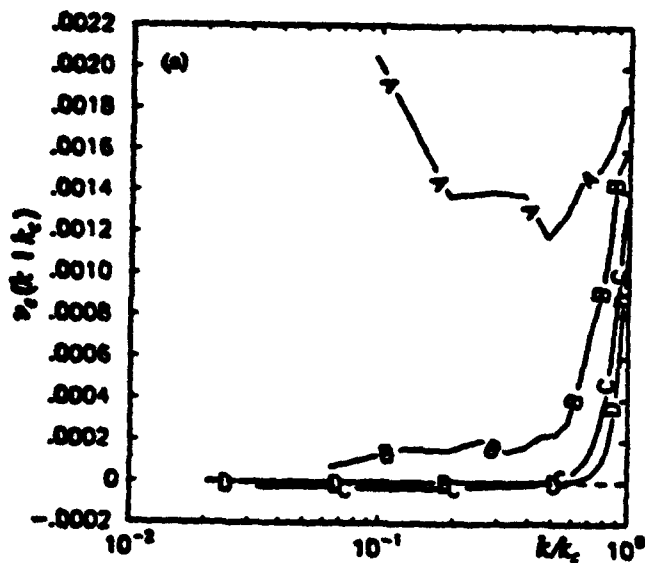


Figure 2. (a) SGS eddy viscosity,  $\nu_e(k; \lambda_e)$ , (b) subgrid energy transfer,  $T^s(k; \lambda_e)$ , and (c) resolved energy transfer,  $T^r(k; \lambda_e)$ , computed from decaying isotropic turbulence DNS data for different  $\lambda_e$ . Curves A-D are  $\lambda_e = 20.5, 25.5, 30.5$  and  $40.5$  respectively. (d) SGS eddy viscosity for forced stationary isotropic turbulence.

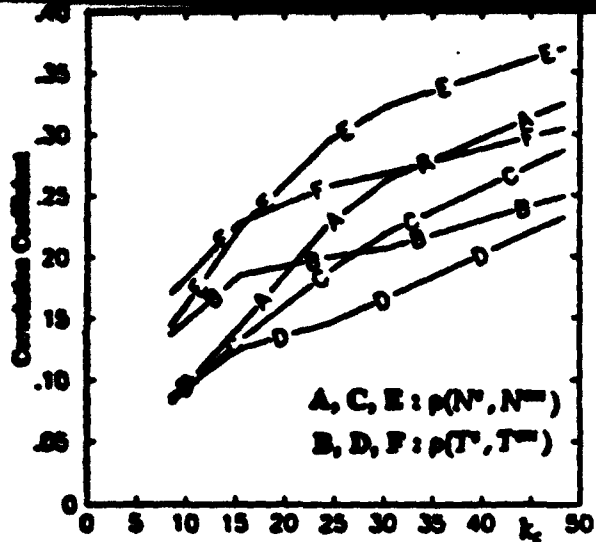
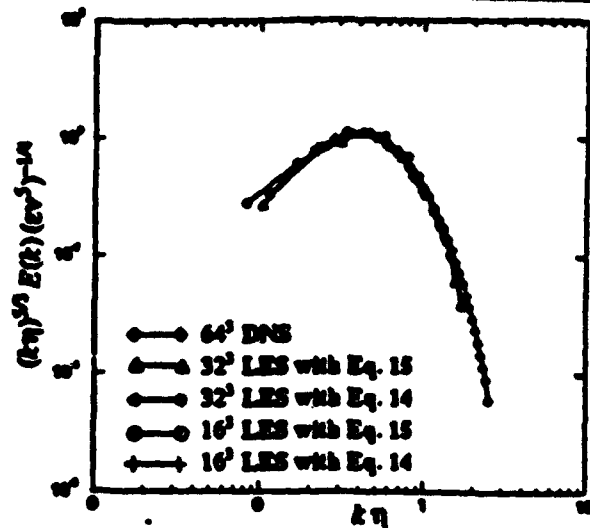
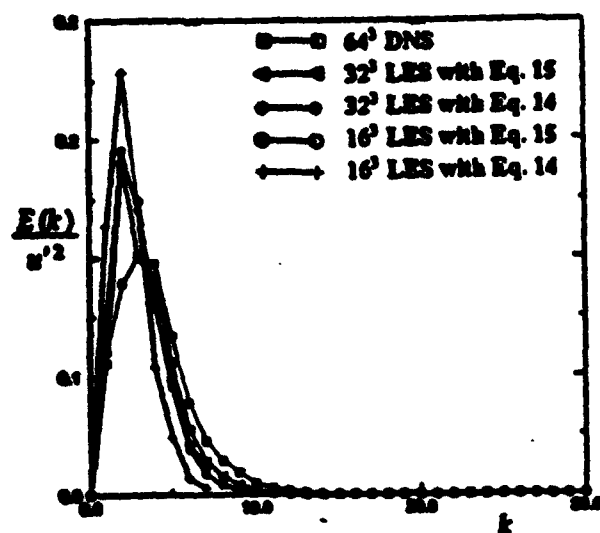


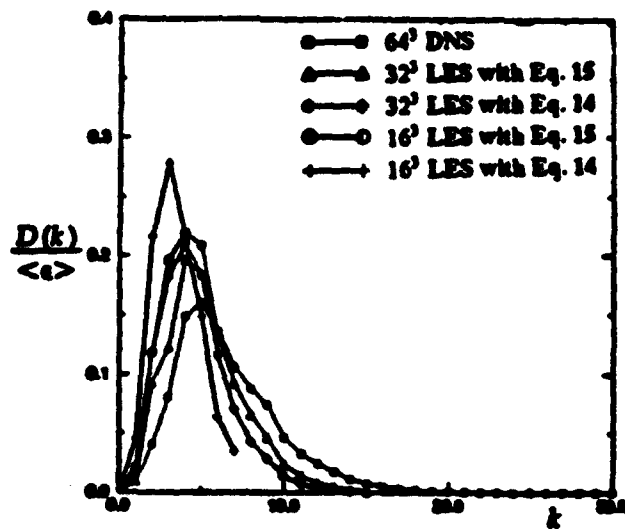
Figure 3. Correlation coefficients between exact and modeled quantities computed in physical space. Lines A, B, E, and F are for the decaying case and lines C and D are for the forced case. Also, lines A, C and E are for the non-linear term while lines B, D and F are for energy transfer.



(a) Kolmogorov scaled energy spectra

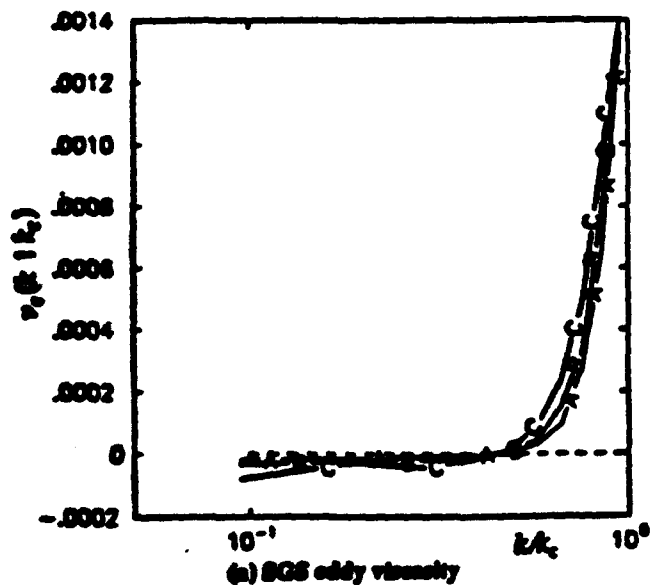


(b) Normalized energy spectra

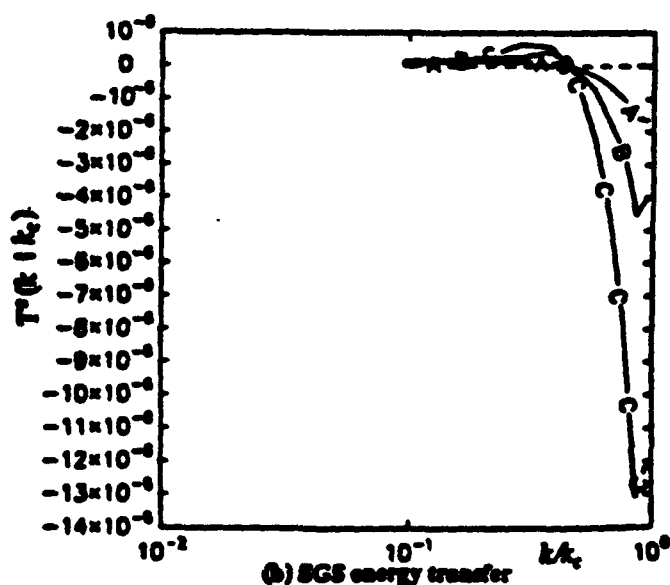


(c) Normalized dissipation spectra

Figure 4. Comparison of the energy and dissipation spectra for the DNS and LES with various models at  $t = 12$  ( $Re_\lambda = 10$ ).



(a) SGS eddy viscosity

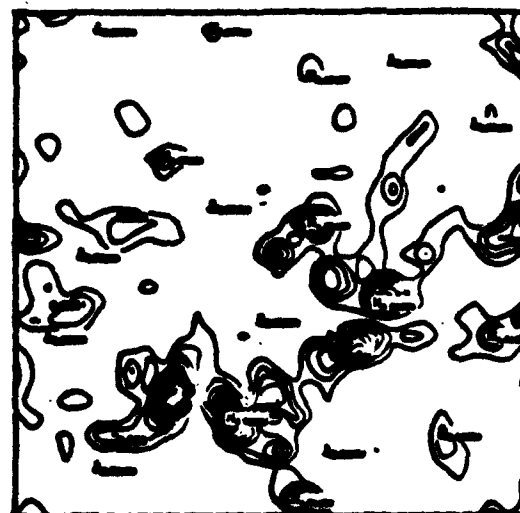


(b) SGS energy transfer

Figure 5. Subgrid eddy viscosity,  $\nu_\epsilon(k/k_c)$  and subgrid energy transfer,  $T^*(k/k_c)$  for  $k_c = 10.5$  for the DNS and LES data. Curve A:  $32^3$  LES with Eq. 14, Curve B:  $32^3$  LES with Eq. 15, Curve C:  $64^3$  DNS.



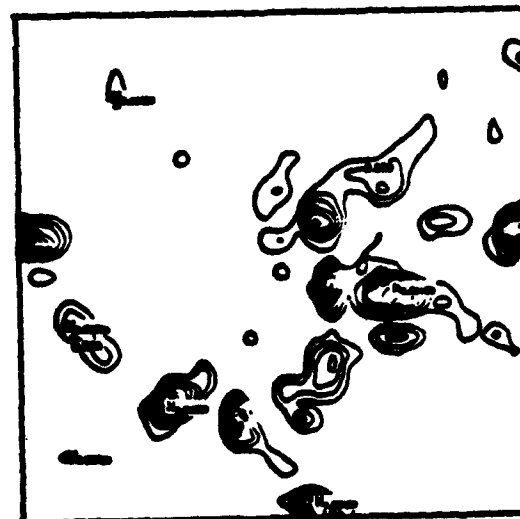
(a) Exact energy transfer from DNS



(b) Energy transfer predicted by Eq. 14

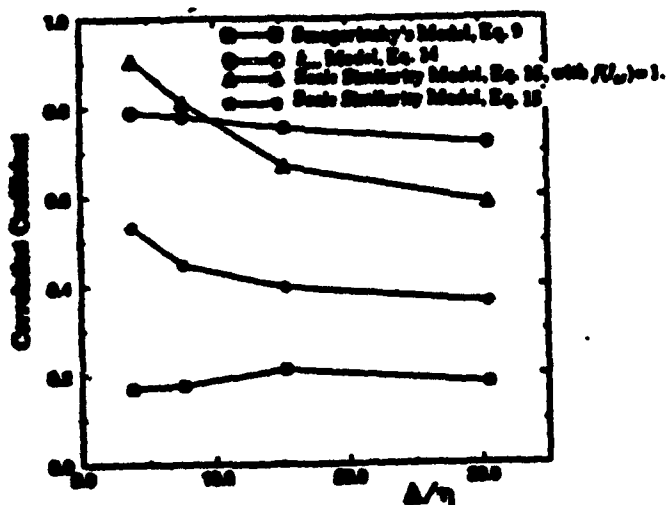


(c) Energy transfer predicted by Eq. 15 with  $f(l_{12}) = 1$ .

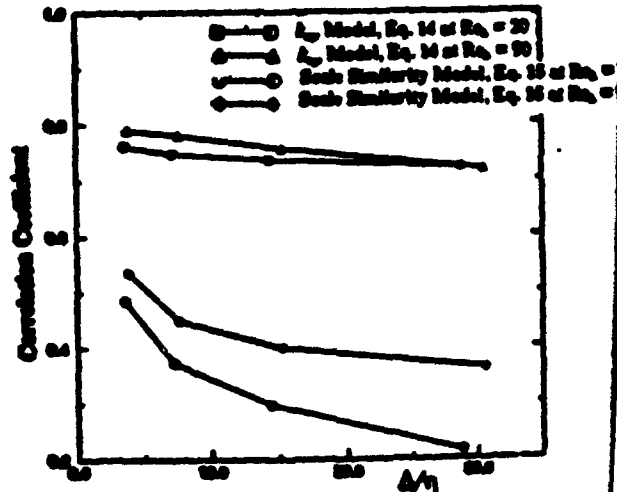


(d) Energy transfer predicted by Eq. 15

Figure 6. Comparison of the contours of the energy transfer for the forced DNS case and the SGS models resolved on  $32^3$  grid. Same contour interval and location for all cases. Solid contours indicate forward scatter and negative contours indicate backscatter.

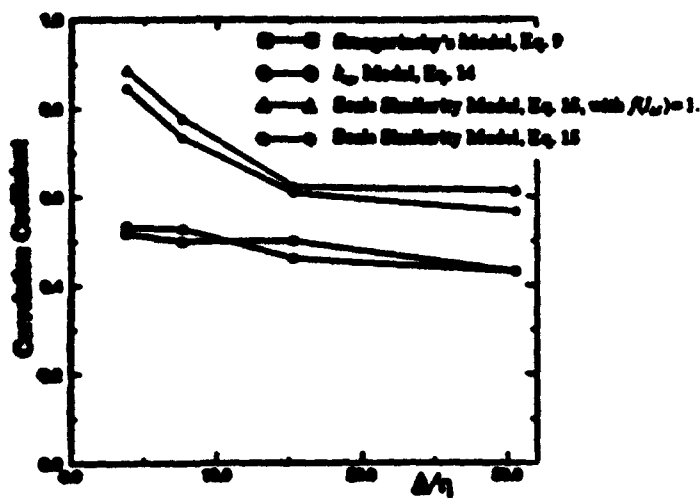


(a) Correlation at  $Re_1 = 90$

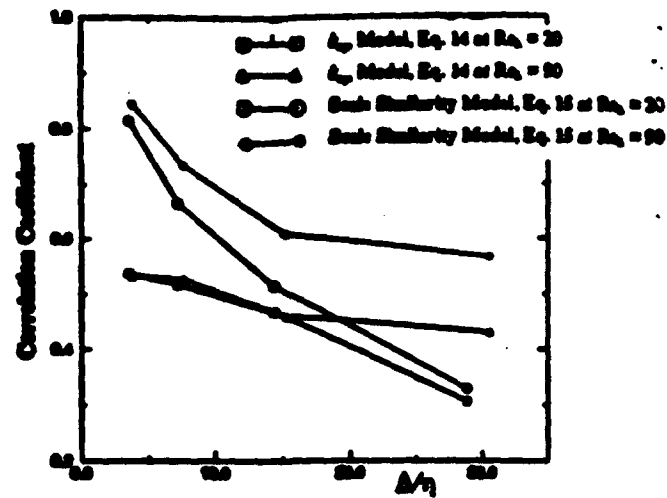


(b) Correlation at  $Re_1 = 90$  and 20

Figure 7. Correlation between the exact stresses from the  $125^3$  DNS data and the stresses computed from the SGS models as a function of filter width.



(a) Correlation at  $Re_\lambda = 90$



(b) Correlation at  $Re_\lambda = 90$  and 20

Figure 8. Correlation between the exact energy transfer from the  $128^3$  DNS data and the energy transfer computed from the SGS models as a function of filter width.

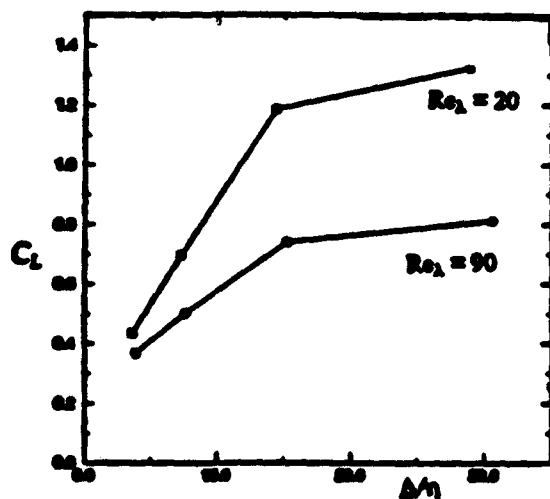


Figure 9. Variation of the coefficient  $c_2$  in the scale similarity model (Eq. 15) with filter width and  $Re_\lambda$

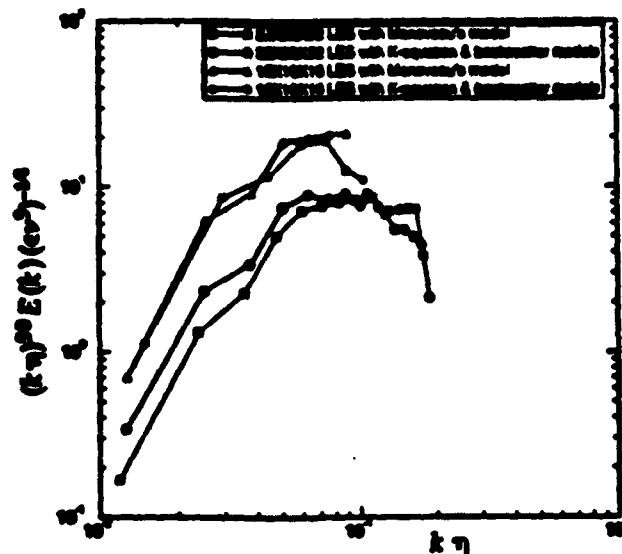
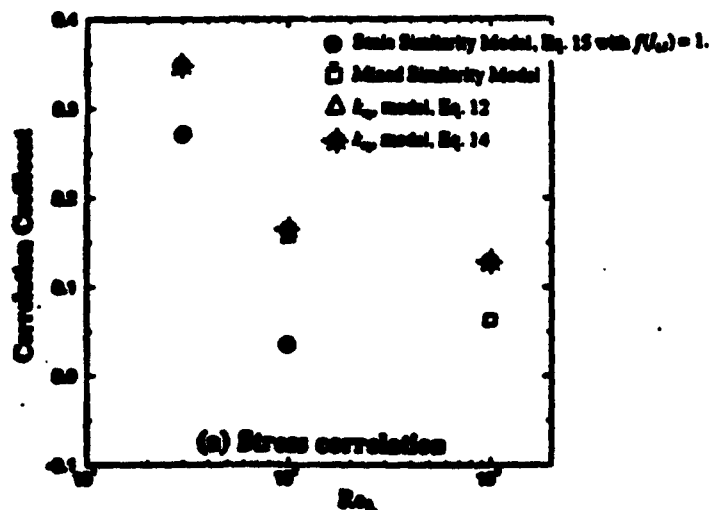
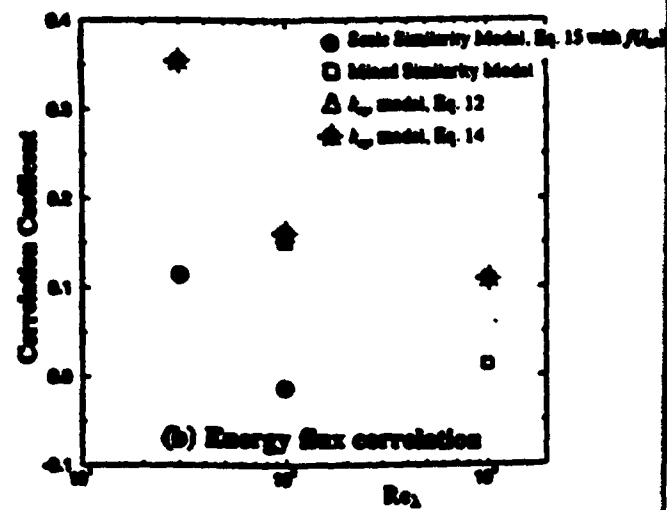


Figure 10. The Kolmogorov scaled energy spectra for  $Re_\lambda = 10^3$ .



(a) Stress correlation



(b) Energy flux correlation

Figure 11. The variation of the stress and energy flux correlations as a function of  $Re_\lambda$  at  $t = 0$ . Correlations computed in the  $16^3$  grid.

AIAA 94-2387

*Extended Abstract Submitted for Presentation at the  
AIAA 25th Fluid Dynamics Conference, June 20-23, 1994  
Colorado Springs, CO*

**EFFECT OF SUBGRID MODELS ON THE COMPUTED INTERSCALE ENERGY TRANSFER  
IN COMPRESSIBLE AND INCOMPRESSIBLE ISOTROPIC TURBULENCE**

**S. Menon**

Associate Professor  
School of Aerospace Engineering  
Georgia Institute of Technology  
Atlanta, Georgia 30332-0150  
(404)-853-9160  
menon@falcon.gatech.edu

and

**P. K. Yeung**

Assistant Professor  
School of Aerospace Engineering  
Georgia Institute of Technology  
Atlanta, Georgia 30332-0150  
(404)-894-9341  
yeung@peach.gatech.edu

**EXTENDED ABSTRACT**

The current state-of-the-art in subgrid models is essentially variants of the simple eddy viscosity model first proposed by Smagorinsky in 1963. This is in spite of the serious limitations of such models that have been brought into attention in recent studies. For example, backscatter of energy from the unresolved to the resolved scales has been observed to occur in direct numerical simulations (DNS) data (Piomelli et al., 1991) clearly demonstrating that the unresolved subgrid processes cannot be modeled by a purely dissipative mechanism. In addition, the "constant" (the Smagorinsky constant) appears to vary from flow to flow and, thus, the subgrid model required further fine-tuning for a specific flow. Recent attempts to improve the eddy viscosity model involves the adaptive evaluation of the subgrid constant (Germano et al., 1991) and an explicit modeling of the subgrid backscatter process (Chamov, 1991). In spite of these developments, it is not yet clear if such simple models are sufficient for large-eddy simulation (LES) of high Reynolds number flows.

The objective of this paper is to evaluate the effect of the form of the chosen subgrid model on the computed interscale energy transfer process between the resolved and unresolved scales in LES. The eventual goal of this research is to develop a subgrid model that will perform adequately in LES of high Reynolds number flows. To investigate the effect of the subgrid model on the interscale energy transfer process, we begin the study by carrying out both DNS and LES for identical flow conditions and then analyzing the energy transfer process using a method developed recently by Domaradzki et al. (1993). They have demonstrated that sub-grid scale (SGS) energy transfer quantities can be readily extracted from DNS data. In incompressible flow, the energy spectrum  $E^L(k)$  of the resolved scales at wavenumber  $k$  evolves by

$$\frac{\partial}{\partial t} E^L(k) = -2\nu k^2 E^L(k) + T(k|k_c) + T^*(k|k_c), \quad k < k_c \quad (1)$$

where  $\nu$  is the kinematic viscosity,  $k_c$  is a cut-off wavenumber separating the resolved and sub-grid scales,  $T(k|k_c)$  represents energy transfer from interactions with resolved scales only, and  $T^*(k|k_c)$  represents interactions with SGS modes. If the form of the spectral SGS eddy viscosity is chosen as



$$\nu_e(k|k_c) = - \frac{T^*(k|k_c)}{2k^2 E^L(k)}, \quad k < k_c \quad (2)$$

then, the behavior of the eddy viscosity as a function of the cutoff wavenumber can be determined, since, in DNS, all terms in equation (1) are known. There are some problems with this approach when LES is considered. In LES, the last term in Equation (1) is modeled by the subgrid model. Thus, the energy transfer process near the cutoff wavenumber will be affected by the form (or choice) of the subgrid model used to represent the effect of the unresolved scales.

This paper will address this particular issue by comparing the results from DNS and LES using various eddy viscosity models such as those studied earlier by Chasnov (1991) and Germano et al. (1991). In addition, a one-equation model for the subgrid turbulent kinetic energy (Ménon, 1992) and a two-equation model for the subgrid turbulent kinetic energy and subgrid helicity (Yoshizawa, 1993) will be evaluated. Higher order subgrid models are considered essential for simulating high Reynolds number flows since, with the available grid resolution the length scales that remain unresolved can contain a significant amount of kinetic energy. In addition, these unresolved scales may be three-dimensional structures. Models that include subgrid helicity (note that, helicity defined as  $\vec{v} \cdot \vec{\omega}$ , is exactly zero for two-dimensional structures) may be able to account for the asymmetry in the subgrid scales. These models will be studied using both spectral and physical space (finite-volume) flow solvers. At present, the method of analysis is similar to that proposed by Domaradzki et al. (1993); however, we hope to develop an equivalent method of analysis that can be used directly in the physical space and will not require transforming the flow field into wavenumber space. This is particularly important since high Reynolds number flows of practical interest occur in complex domains (e.g., rearward facing steps) and, thus, it will not be possible to evaluate the energy transfer using Fourier transforms.

In this paper, we consider the energy transfer properties of decaying incompressible and compressible isotropic turbulence. In the following, we show and compare preliminary results obtained by four different methods: DNS using the constant-density pseudo-spectral algorithm of Rogallo (1981), DNS using a compressible finite-volume code (Ménon, 1992) at low Mach number, LES using a compressible eddy viscosity model in the finite-volume code, and LES using a finite-difference incompressible code. The DNS and LES data are obtained with  $64^3$  and  $32^3$  grid points, respectively. Except for differences in numerical resolution and methods, the parameters are chosen to simulate statistically the same flow in all cases. More details of the numerical methods and the subgrid models will be given in the final paper.

Beginning from a isotropic Gaussian random field with a specified initial energy spectrum, the hydrodynamic field is allowed to evolve until a "realistic" self-similar state is developed (as in Yeung and Brasseur 1991). Results from a  $64^3$  calculation show a power-law decay of energy, with exponent 1.31 consistent with grid-generated turbulence data, and small-scale universality illustrated by the collapse of high-wavenumber spectra at different times under Kolmogorov scaling, as shown in Figures 1a-d. It is interesting to note that both the DNS results agree remarkably well and, furthermore, that the LES data also shows very good agreement with the DNS data.

The flow fields at various times were analyzed. Here, the result obtained at a time  $t=9.0$  (which corresponds to around 20.5 initial eddy-turnover times) was selected for further analysis. By this time, the turbulence is well developed, and the Taylor-scale Reynolds number (based on the r.m.s. velocity and Taylor microscale) is approximately 11 (slowly decreasing with time). Figures 2a - 2d shows the shapes of the normalized energy and dissipation spectra at the chosen time for the four different cases. The DNS data from both simulations are well resolved and also agree with each other remarkably well. The peaks of energy and dissipation spectra are separated by a factor of two. The LES data also agrees reasonably with the DNS results, however, the peak value of both the energy and dissipation is slightly higher.

Figures 3, 4 and 5 show the eddy viscosity (Equation (2)), subgrid transfer,  $T^*(k|k_c)$  and resolved transfer  $T(k|k_c)$ , respectively, for different cutoff wavenumbers,  $k_c$ . Although the range of scales available in our  $64^3$  calculations is limited, nevertheless, some interesting conclusions may be drawn, to be confirmed by  $128^3$  results that will be obtained by the time of the Symposium. Results for the lowest cut-off chosen ( $k_c = 5$ ) are somewhat erratic, because they correspond to LES with a very coarse filter, and because of statistical variability associated with the resolved-scale energy spectrum ( $E^L(k)$ ) at low

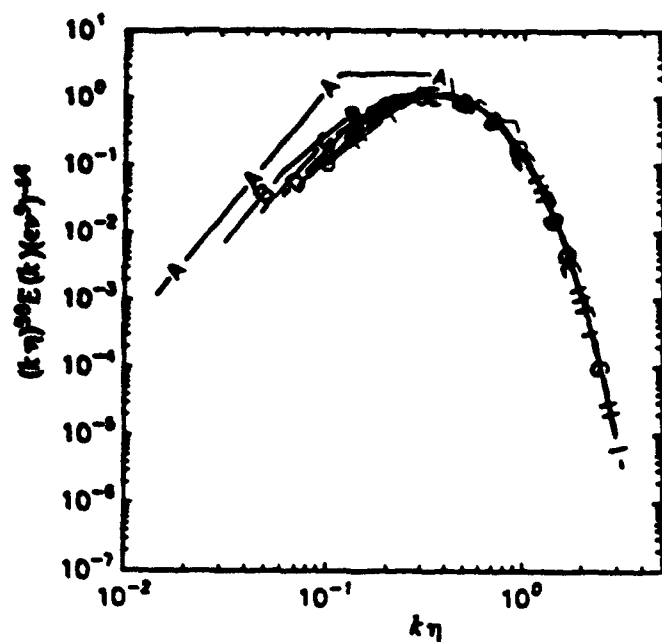
wavenumbers. For higher cutoffs, spectral eddy viscosity increases sharply as the cutoff wavenumber is approached (Figure 3a-c). Note that for the LES case (Figure 3c), the cutoff wavenumber  $k_c=15$  is actually the maximum wavenumber in the resolved field. At small  $k/k_c$ , the spectral eddy viscosity is negative, showing an inherent limitation of the eddy viscosity concept itself. These features are consistent with the results of Domaradzki et al. (1993), who studied a Taylor-Green vortex and presented the variation of  $\nu_e(k|k_c)$ , but not the transfers ( $T(k|k_c)$  and  $T^*(k|k_c)$ ) as a function of  $k/k_c$ .

Figure 4 shows that the effect of sub-grid scales is mainly to extract energy from the large scales, but there is also a non-negligible backscatter ( $T^*(k|k_c) > 0$ ) effect acting on the largest scales. We plan to study further this effect by explicitly modeling the backscatter process as done earlier by Chasnov (1991). Figure 5 shows that the nature of interactions among the resolved scales themselves is primarily forward cascading: with energy loss ( $T(k|k_c) < 0$ ) at low  $k/k_c$  and energy gain ( $T(k|k_c) > 0$ ) as  $k/k_c$  approaches unity.

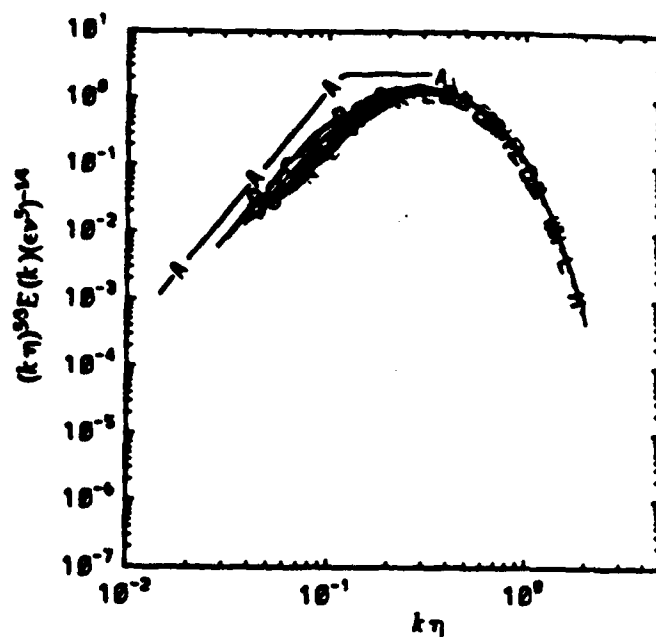
These results will be further validated for the final paper by carrying out  $128^3$  DNS simulations. As noted above, subgrid models, such as the eddy viscosity model with adaptive evaluation of the constant (Germano et al., 1991) and the one-equation and two-equation models, will be implemented in both the finite-volume codes and the effect of the subgrid model on the energy transfer process will be investigated in detail using a series of LES at various grid resolution. The effect of increasing the Reynolds number will also be investigated. The results of these studies should shed light on the deficiencies and strengths of the subgrid models and provide a direction for improving the models so that high Reynolds number flows can be simulated.

## REFERENCES

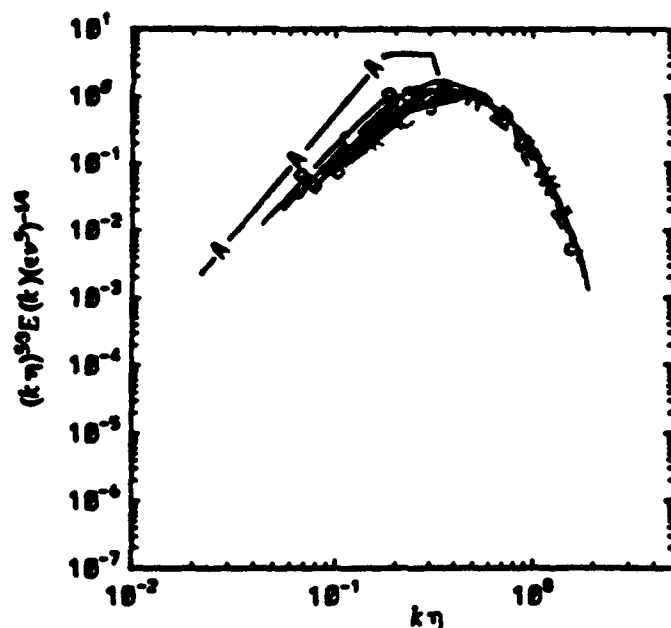
- Chasnov, J. R. (1991) "Simulation of the Kolmogorov inertial subrange using an improved subgrid model," *Phys. Fluids A*, Vol. 3, pp. 188.
- Domaradzki, J. A., Liu, W., and Brachet, M. E. (1993) "An Analysis of subgrid scale interactions in numerically simulated isotropic turbulence", *Phys. Fluids A*, Vol. 5, pp. 1747.
- Germano, M., Piomelli, U., Moin, P., and Cabot, W. H. (1991) "A dynamic subgrid-scale eddy viscosity model," *Phys. Fluids A*, Vol. 3, pp. 1760.
- Menon, S. (1992) "Secondary fuel injection control of combustion instability in a ramjet", to appear in *Combustion Science and Technology*.
- Piomelli, U., Cabot, W. H., Moin, P., and Lee, S. (1991) "Subgrid-scale backscatter in turbulent and transitional flows," *Phys. Fluids A*, Vol. 3, pp. 1766.
- Rogallo, R. S. (1981) "Numerical experiments in Homogeneous Turbulence," NASA TM 81315.
- Yeung, P. K. and Brasseur, J. G., (1991) "The response of isotropic turbulence to isotropic and anisotropic forcing at the large scales," *Phys. Fluids A*, Vol. 3, pp. 884.
- Yoshizawa, A. (1993) "Bridging between Eddy-Viscosity Type and Second-Order Models using a Two-Scale DIA" Symposium on "Turbulent Shear Flows", Japan, August 16-18.



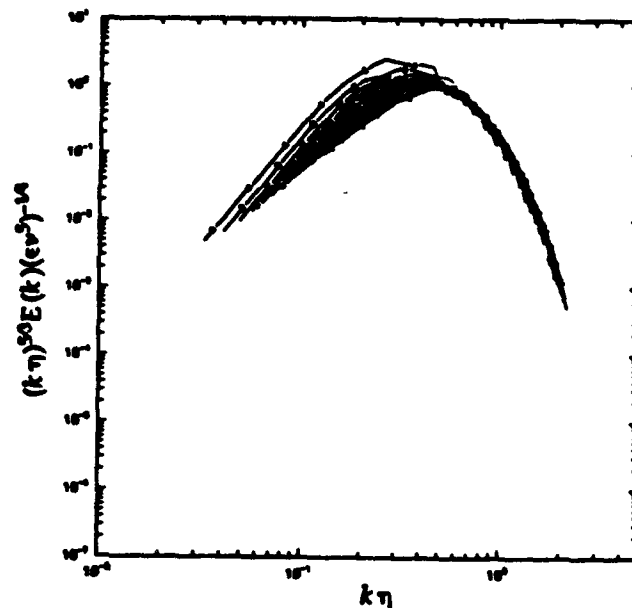
(a) DNS,  $64^3$ , spectral method



(b) DNS,  $64^3$ , finite-volume method



(c) LES,  $32^3$ , finite-volume method



(d) LES  $32^3$ , finite-difference method, incompressible

Figure 1. Temporal development of the Kolmogorov-scales energy spectrum during decay from an initially Gaussian state. The spectra are shown at various times and show that the spectra collapse at high wave numbers under Kolmogorov scaling.

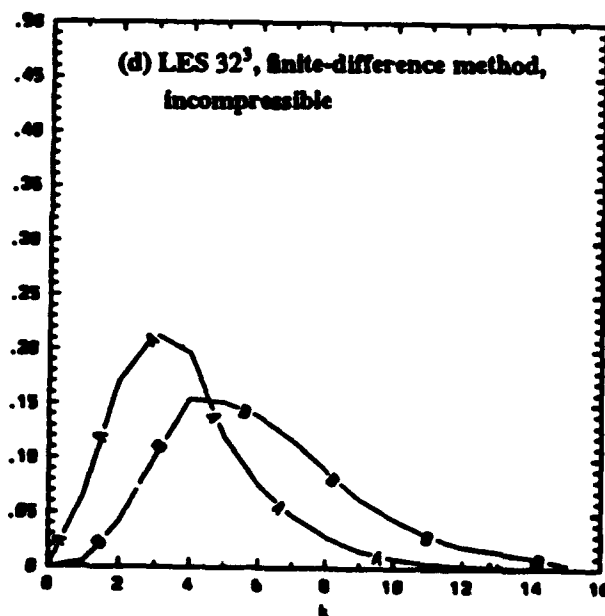
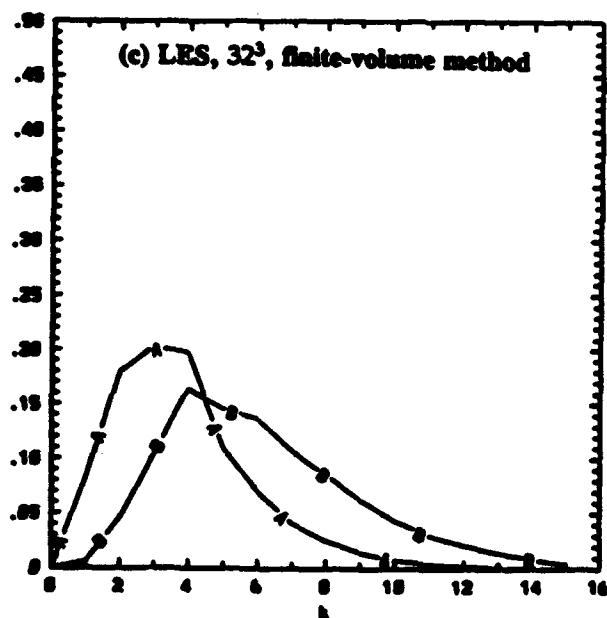
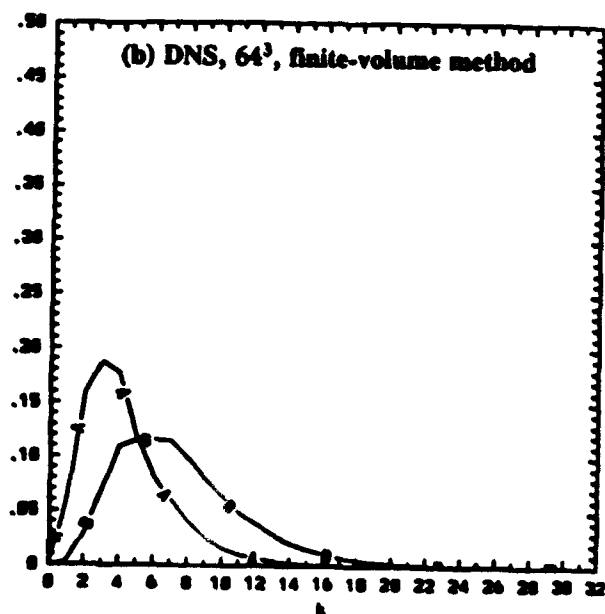
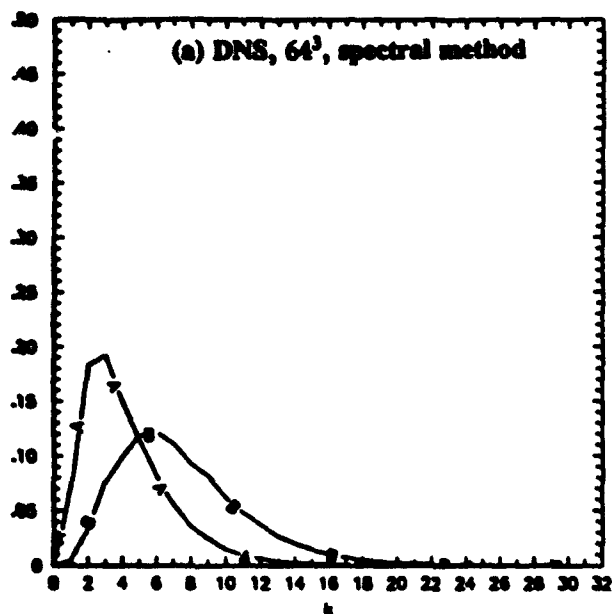


Figure 2. Normalized energy and dissipation spectra

CURVE A:  $E(k)/\bar{u}^2$

B:  $D(k)/\langle \epsilon \rangle$

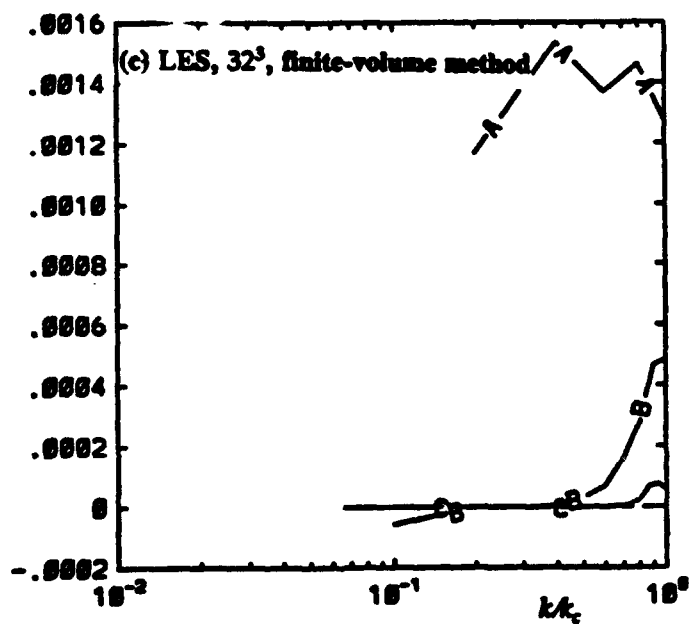
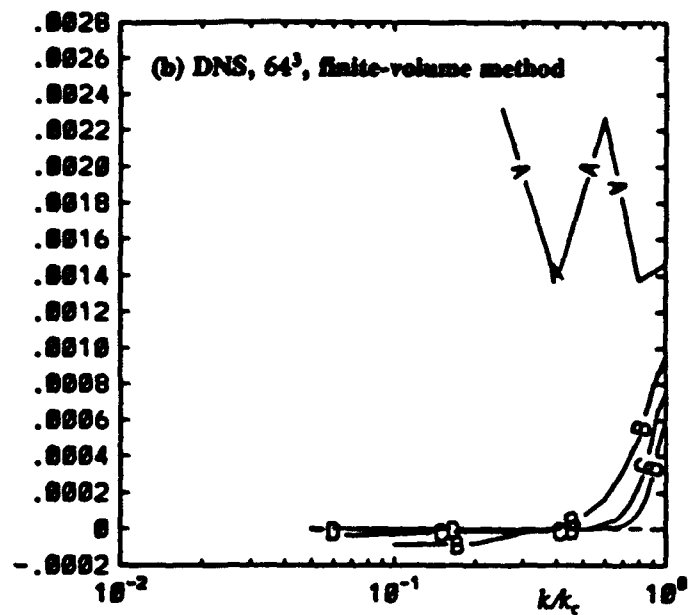
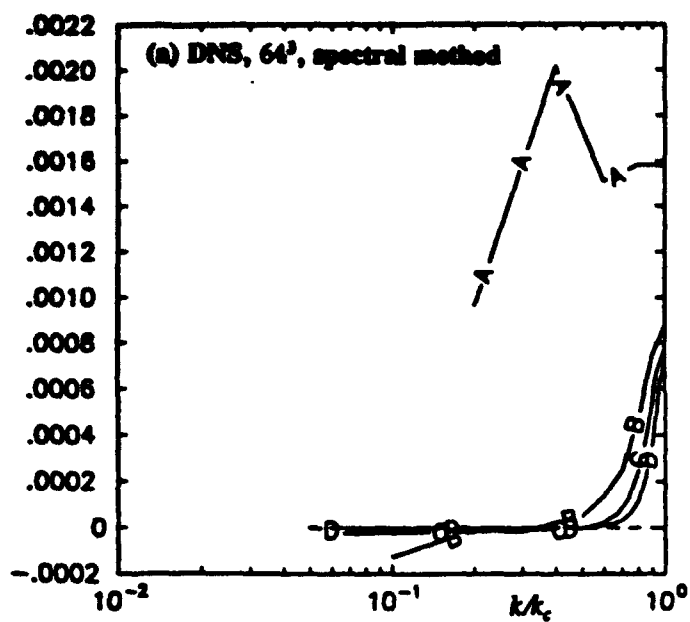


Figure 3. Spectral subgrid-scale eddy viscosity for various cutoff wavenumber.

Curves A :  $k_c = 5$ , B :  $k_c = 10$ , C :  $k_c = 15$ , D :  $k_c = 20$ .

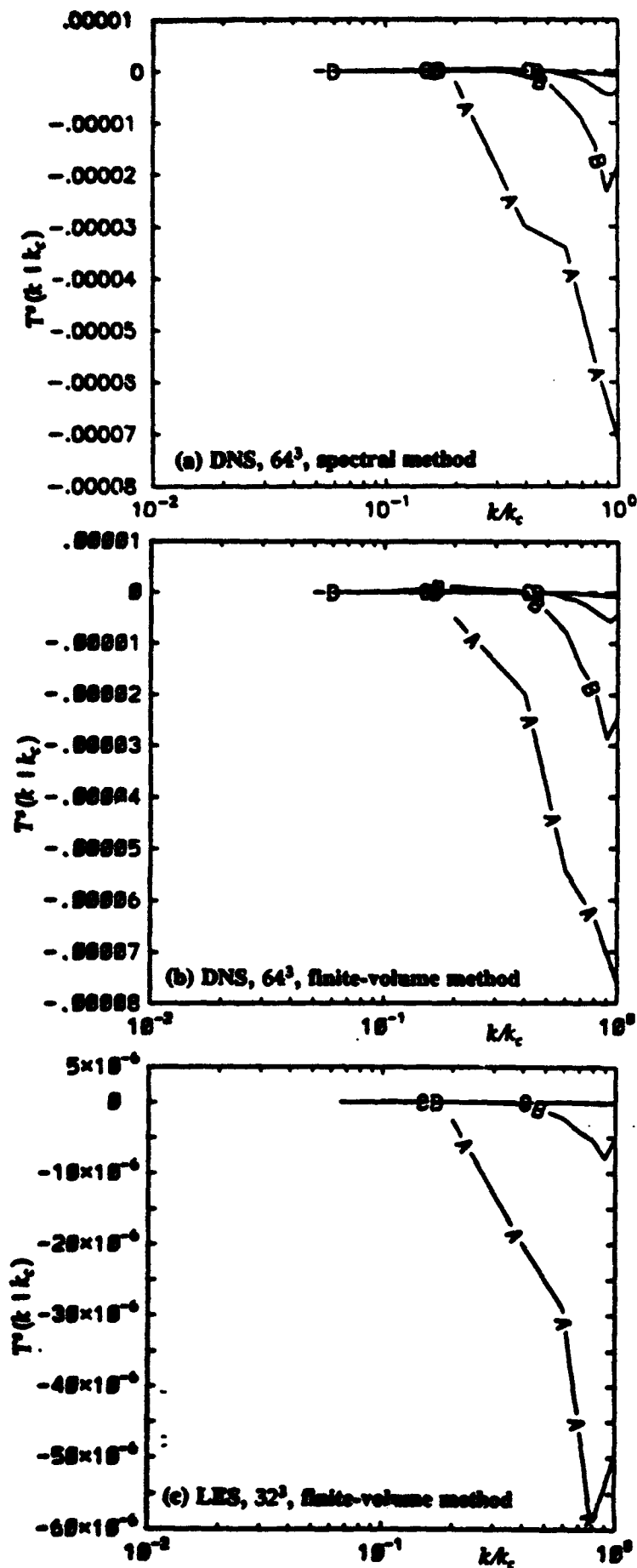


Figure 4. Energy transfer from interactions with the unresolved subgrid scales. Curves A-D, as in figure 3.

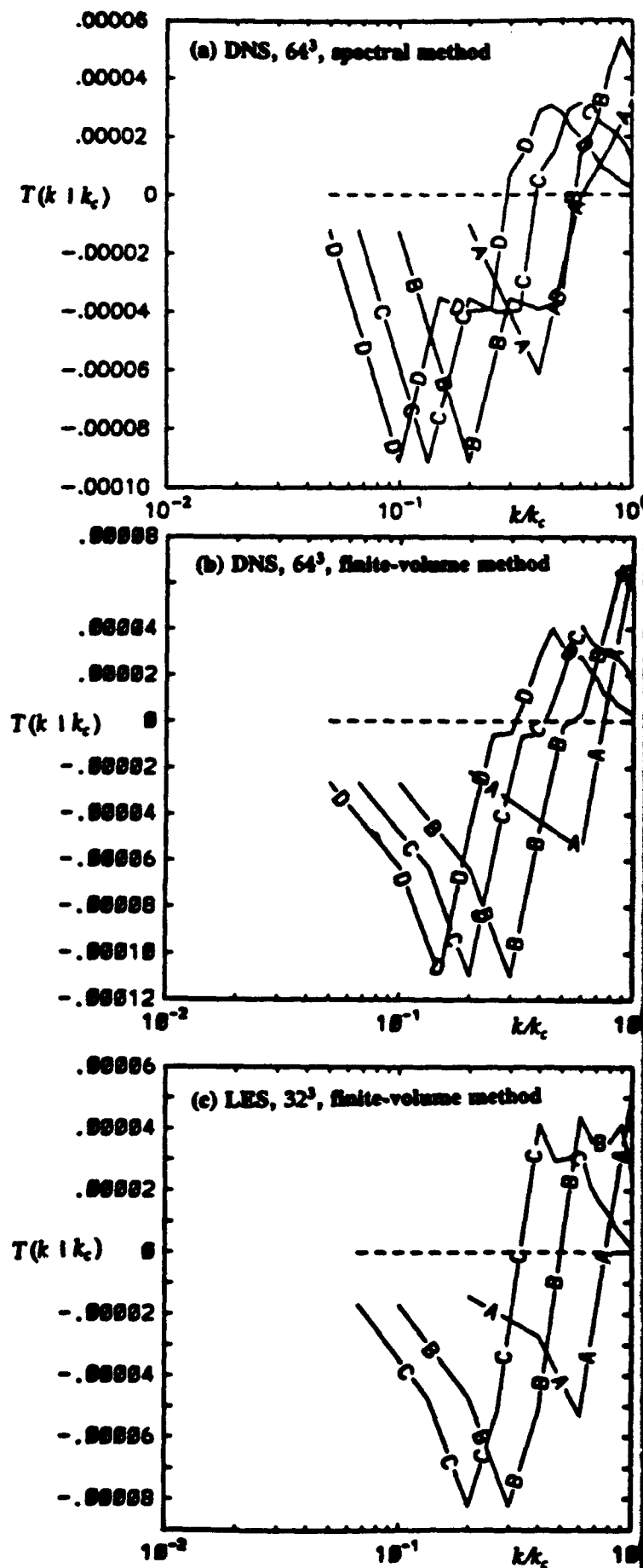


Figure 5. Energy transfer from interactions with the resolved scales. Curves A-D, as in figure 3.

**A NEW DYNAMIC ONE-EQUATION SUBGRID MODEL  
FOR LARGE EDDY SIMULATIONS**

**Wen-Week Kim, Suresh Menon and Veerathu K. Chakravarthy  
School of Aerospace Engineering  
Georgia Institute of Technology  
Atlanta, Georgia 30332-0150**

**1. INTRODUCTION**

The dynamic subgrid scale (SGS) modeling technique, introduced by Germano *et al.* (1991), has been successfully applied to various types of flow fields (see Moin *et al.*, 1994 for a recent review). There are three important features of this modeling approach. First, the model *constant*, the so-called Smagorinsky's constant, is not prescribed *a priori*, rather, it is determined as a part of the solution. This approach removed one of the major problems associated with the Smagorinsky's eddy viscosity model which was the determination (and fine-tuning) of the constant for different flows. Second, the dynamic model shows the correct asymptotic behavior near walls and third, as a result of the dynamic evaluation, the *constant* can become negative in certain regions of the flow field and thus, appears to have the capability to mimic backscatter of energy from the subgrid scales to the resolved scales. This last feature is particularly attractive since direct numerical simulation (DNS) data has shown that backscatter effect can dominate over a significant portion of the grid points in the flow field (e.g., Piomelli *et al.*, 1991). However, large-eddy simulations (LES) using this dynamic model has shown that the backscatter effect of Germano's model can be excessive and can cause numerical instability. Some recent efforts (Moin *et al.*, 1994; Piomelli and Liu, 1994) were directed particularly to develop better methods to evaluate the *constant*. However, these studies still assume that the form of the eddy viscosity, as proposed by Smagorinsky, is still appropriate and valid for the entire range of flows. Recent DNS studies of decaying isotropic turbulence suggest that the assumption of the local equilibrium between the SGS energy production and dissipation rate (which was used to derive the Smagorinsky model) may not be satisfied over a large portion of the grid points. This lack of local equilibrium can be significant when the flow fields at different grid resolutions are related to each other, as is the case in the dynamic model.

In this paper, these issues are addressed by considering two new subgrid models that do not require local equilibrium between the SGS energy production and dissipation rate. These models have been developed using the dynamic modeling approach and therefore, there are no *constants* that have to be prescribed *a priori*. The first model that is studied is a dynamic version of the Kolmogorov's scaling expression for eddy viscosity and the second model is a one-equation model for SGS kinetic energy.

Using LES of decaying isotropic turbulence at various Reynolds number, the behavior of these new dynamic models have been compared to the predictions of the dynamic model based on the Smagorinsky's eddy viscosity concept. An eventual goal of this research is to determine

the form of a dynamic subgrid model that will provide realistic results over a wide range of Reynolds number and grid resolution.

The numerical simulations were carried out using a finite-difference code that is second-order accuracy in time and fifth-order (the convective terms) and sixth-order (the viscous terms) accuracy in space using upwind-biased differences (Rai and Moin, 1991). Time-accurate solutions of the incompressible Navier-Stokes equations are obtained by the artificial compressibility approach (Rogers *et al.*, 1991) which requires subiteration in pseudotime to get the divergence-free flow field. Earlier (Menon and Yeung, 1994), this code was validated by carrying out DNS of decaying isotropic turbulence and comparing the resulting statistics with the predictions of a well known pseudo spectral code (Rogallo, 1981).

## 2. DYNAMIC SUBGRID MODELING

In the following, the forms of the dynamic subgrid models studied here are briefly described. More details of the modeling approach will be given in the final paper.

### 2.1 Dynamic Smagorinsky Model

The primary requirement in LES is the modeling of the SGS stresses that result from the spatial filtering of the instantaneous incompressible Navier-Stokes equations. If an appropriate filter is employed (here, a top hat filter with a filter width  $\bar{\Delta}$  is used, where,  $\bar{\Delta}$  is the grid spacing), then the true SGS stress tensor is:  $\tau_{ij} = u_i u_j - \bar{u}_i \bar{u}_j$ . This stress tensor must be modeled to close the LES equations of motion. The Smagorinsky eddy viscosity closure for the SGS stress tensor is of the form:

$$\tau_{ij} - \frac{1}{3} \delta_{ij} \tau_{kk} = -2 \nu_T \bar{S}_{ij} \quad , \quad \nu_T = C \bar{\Delta}^2 |\bar{S}| \quad (1)$$

where  $C$  is the model coefficient,  $\bar{S}_{ij}$  is the resolved scale strain rate tensor

$$\bar{S}_{ij} = \frac{1}{2} \left( \frac{\partial \bar{u}_i}{\partial x_j} + \frac{\partial \bar{u}_j}{\partial x_i} \right) \quad (2)$$

and  $|\bar{S}| = (2 \bar{S}_{ij} \bar{S}_{ij})^{1/2}$ . Here, the overbar on the flow variables indicates the result of filtering at the grid scale  $\bar{\Delta}$ . In the dynamic modeling approach, a mathematical identity between the stresses resolved at the grid scale filter  $\bar{\Delta}$  and a test filter  $\hat{\Delta}$  (typically chosen to be twice of the grid filter  $\bar{\Delta}$ ) is used to determine the model coefficient  $C$  as a part of the simulation. Thus, if the application of the test filter on any variable  $\phi$  is denoted by  $\hat{\phi}$  or  $\langle \phi \rangle$ , then it can be shown that

$$L_{ij} = T_{ij} - \hat{\tau}_{ij} = \langle \bar{u}_i \bar{u}_j \rangle - \hat{\bar{u}}_i \hat{\bar{u}}_j \quad (3)$$



Here,  $T_y (= \langle \overline{u_i u_j} \rangle - \hat{u}_i \hat{u}_j)$  is defined by using the test filter. Using the assumption of the self-similarity of the subgrid stress,  $T_y$  can be modeled in the same way as  $\tau_y$  resulting in the following expression:

$$T_y - \frac{1}{3} \delta_{ij} T_{kk} = -2 \nu_T \hat{S}_{ij}, \quad \nu_T = C \hat{\Delta}^2 |\hat{S}| \quad (4)$$

Substituting (1) and (4) into (3), one can obtain an equation for  $C$

$$L_y - \frac{1}{3} \delta_{ij} L_{kk} = 2 C M_y \quad (5)$$

where

$$M_y = - \left( \hat{\Delta}^2 |\hat{S}| \hat{S}_{ij} - \overline{\Delta^2 |\bar{S}| \bar{S}_{ij}} \right) \quad (6)$$

Equation (5) is a set of  $n(n+1)/2$  independent equations for one unknown  $C$ . To minimize the error from solving this overdetermined system, Lilly (1992) proposed a least square method which yields

$$C = \frac{1}{2} \frac{L_y M_y}{M_y M_y} \quad (7)$$

Past studies (e.g., Zang *et al.*, 1992; Yang and Ferziger, 1993) using this approach have shown that the value of  $C$  obtained from Equation (7) can vary widely in the flow field. This can cause numerical instability. To relieve this problem, spatial averaging is typically performed for both the numerator and the denominator on the RHS of (7) (Piomelli, 1993). Usually, this averaging is done only in the directions of flow homogeneity (e.g., Moin *et al.*, 1991). In the present study of homogeneous isotropic turbulence, averaging is implemented over the entire computational domain, hence  $C$  is a function of time only.

## 2.2 Dynamic Kolmogorov Scaling Model

Recently, Wong and Lilly (1994) reevaluated the Kolmogorov's scaling expression for the eddy viscosity. The representative variables characterizing SGS fluctuations are the SGS energy dissipation rate  $\varepsilon$  and the SGS length scale which can be approximated by the grid interval  $\Delta$ . Using dimensional arguments, the subgrid eddy viscosity can be written as,

$$\nu_T = C_\varepsilon \bar{\Delta}^{4/3} \quad (8)$$

Here, the model coefficient  $C_\varepsilon$  has the dimension related to  $\varepsilon$  (precisely,  $C_\varepsilon = \varepsilon^{1/3}$ ). This simple expression for  $\nu_T$  can be robust because it does not employ the assumption of local equilibrium between SGS energy production rate and dissipation rate which was adopted to derive the Smagorinsky model (and which is implicit in the dynamic model described in Section 2.1). Another advantage of this model is that, due to the simplicity of the model, the total

computational time can be significantly reduced. However, this model can be valid only by employing a dynamic modeling method to determine the model coefficient. Otherwise, there may be no way to prescribe this non-dimensionless coefficient by a fixed value. The resulting equation for  $C_\epsilon$  is expressed as follows,

$$L_i - \frac{1}{3} \delta_{ij} L_{kk} = -2 C_\epsilon (\hat{\Delta}^{4/3} - \bar{\Delta}^{4/3}) \hat{S}_{ij} \quad (9)$$

### 2.3 Dynamic $k$ -equation Model

A higher order model is also considered in this study. This is a one equation model for the SGS kinetic energy  $k$  ( $\equiv (\overline{u_i^2} - \bar{u}_i^2)/2$ ). This model was recently evaluated by Menon and Yeung (1994) through *a priori* tests using DNS of decaying and forced isotropic turbulence. In this model, an evolution equation for  $k$  can be written in the following form

$$\frac{\partial k}{\partial t} + \bar{u}_i \frac{\partial k}{\partial x_i} = -\tau_{ij} \frac{\partial \bar{u}_i}{\partial x_j} - \epsilon + \frac{\partial}{\partial x_i} \left( \nu_T \frac{\partial k}{\partial x_i} \right) \quad (10)$$

where

$$\tau_{ij} = -2 \nu_T \bar{S}_{ij} + \frac{2}{3} \delta_{ij} k \quad , \quad \nu_T = C_\nu k^{1/2} \bar{\Delta} \quad (11)$$

Also, one can model the dissipation rate  $\epsilon$  ( $\equiv \nu \left[ \overline{(\partial u_i / \partial x_j)^2} - (\partial \bar{u}_i / \partial x_j)^2 \right]$ ) using  $k$ , as

$$\epsilon = C_\epsilon \frac{k^{3/2}}{\bar{\Delta}} \quad (12)$$

Menon and Yeung (1994) chose the model coefficients, based on an earlier study (Yoshizawa, 1993), to be  $C_\nu=0.0854$  and  $C_\epsilon=0.916$ . However, these values were found to cause excessive dissipation of large-scale energy for isotropic turbulence. In the present study, we apply the dynamic modeling technique to obtain appropriate values of the coefficients. To implement the dynamic approach, the subgrid kinetic energy  $K$  at the test filter level is required. This is obtained by using the trace of (3),  $K = L_{ii} / 2 + \hat{k}$ . Thus, using the procedure described earlier, equations for both  $C_\nu$  and  $C_\epsilon$  can be derived:

$$L_i - \frac{1}{3} \delta_{ij} L_{kk} = -2 C_\nu (\hat{\Delta} K^{1/2} \hat{S}_{ij} - \bar{\Delta} \langle k^{1/2} \bar{S}_{ij} \rangle) \quad (13)$$

$$\nu \left( \left\langle \frac{\partial \bar{u}_i}{\partial x_j} \frac{\partial \bar{u}_i}{\partial x_j} \right\rangle - \frac{\partial \hat{u}_i}{\partial x_j} \frac{\partial \hat{u}_i}{\partial x_j} \right) = C_\epsilon \left( \frac{K^{3/2}}{\bar{\Delta}} - \frac{\langle k^{3/2} \rangle}{\bar{\Delta}} \right) \quad (14)$$

Here, equation (14) is a scalar equation for a scalar unknown and thus, we can obtain the exact value for  $C_\epsilon$  without applying the least square method.

One may think that the merit of the LES approach lies in the simplicity of the model used for the simulations and that, this merit may be lost by using the higher-order models such as the one-equation model. However, the increased cost of this type of model is compensated by the improvement in the accuracy resulting by not assuming local balance between the SGS energy production and dissipation rate. According to our *a priori* test using relatively high resolution DNS (using  $128 \times 128 \times 128$  and  $64 \times 64 \times 64$  grid resolutions), over a large portion of the grid points in isotropic turbulent flow, local equilibrium assumption is violated. This implies that models that do not require local equilibrium such as the one-equation model has the potential to produce better results than the Smagorinsky-type model. The earlier studies using the one-equation model with fixed values of the coefficients (Menon and Yeung, 1994) improved the results when compared to the Smagorinsky's model with fixed value of coefficient. However, the results were poorer than the results obtained using the dynamic Smagorinsky's model. Analysis of the simulation data showed that this was due to a poor prediction of both the production and dissipation terms in (10) using fixed coefficients. Especially, the prediction of the dissipation terms was very poor. In the present study, the use of the dynamic procedure to evaluate the coefficients results in a much better prediction of both the production and dissipation terms in the k-equation model. This in turn improves significantly the results of the LES using the dynamic k-equation subgrid model.

### 3. PRELIMINARY RESULTS AND DISCUSSION

To evaluate the three different dynamic SGS models (described in Sec. 2), LES of decaying homogeneous isotropic turbulence were conducted. Starting from an initially divergent free velocity field with a prescribed energy spectrum, the flow is allowed to develop into realistic decaying turbulence. The flow under consideration is modeled in a cubic box with periodic boundary conditions, and two grid resolutions,  $32 \times 32 \times 32$  and  $16 \times 16 \times 16$ , were employed for the simulations. The simulations were performed for three different initial Taylor Reynolds numbers  $Re_\lambda = 30, 100$  and  $1000$ . In the following, preliminary results are discussed to highlight the behavior of the new dynamic subgrid models. The results discussed here are obtained by using the flow field at an instant in time where the flow field has relaxed to a realistic decaying turbulence and the Reynolds number of the flow field is decreasing very slowly.

To evaluate the self consistency of the dynamic models, the LES results obtained on the  $32 \times 32 \times 32$  grid resolution were compared to the LES results obtained on the  $16 \times 16 \times 16$  grid. To ensure that both grid resolution simulations are being performed using nearly identical initial conditions, the initial flow field for the  $16 \times 16 \times 16$  grid simulation is obtained by filtering the  $32 \times 32 \times 32$  grid resolved flow field. The resulting flow fields from these two different resolution simulations can be related using the mathematical identity, (3). By this approach, the modeled quantity  $\overline{u_i u_j}$  can be obtained from the two data sets which should be identical or at least highly correlated if the subgrid model performed correctly at the two grid levels. To quantify the behavior of the subgrid model, correlation coefficients (defined in the usual manner) are computed using the anisotropic parts of expressions for  $\overline{u_i u_j}$ . The variation of the averaged correlation coefficients of these three anisotropic components are shown in Fig. 1 as a function of the Taylor Reynolds number at the instant of the comparison. The correlation coefficient is very high for all the models over the entire range of Taylor Reynolds numbers. However, the

correlation coefficient for the dynamic Smagorinsky model decreases with increase in the Reynolds numbers. Although the correlation coefficient for the dynamic Kolmogorov scaling model is always higher than the others, it was found using spectral space analysis that this model has some problems in predicting the dissipation rate of the SGS turbulent energy. This model is more dissipative in the earlier transitional stage and less dissipative in the fully developed turbulent stage. This problem may be caused by the lack of direct modeling of the dissipation rate when the Kolmogorov's scaling for the eddy viscosity is used. In any event, the results shown in Fig. 1 clearly suggest that the models that do not make the assumption of local equilibrium between the production and dissipation rate produce better results than the dynamic Smagorinsky's model. This is important since the eventual goal of LES methodology is to develop subgrid models that will allow simulation of high Reynolds number flows using relatively coarse grids (grid resolution restrictions are typically imposed due to computer resource limitations).

Fig. 2a shows the variation in the dynamically evaluated constants with time during the simulation for  $Re_{\lambda} = 100$  and Fig. 2b shows the variation of the model constant with the Taylor Reynolds numbers. Obviously, the model coefficients go through changes in the earlier transitional stage. However, after some time, all coefficients reach an asymptotic state with the exception of  $C_\epsilon$  in Kolmogorov's scaling expression which keeps decreasing as the kinetic energy decreases. Also, the values of the coefficients at this asymptotic state are almost independent on Reynolds number except for  $C_\epsilon$  in  $k$ -equation model because  $\epsilon$ , and hence  $C_\epsilon$ , which is generated from direct modeling of  $\epsilon$ , is very sensitive to the grid resolution and Reynolds number. The resulting constants are similar to the values obtained in earlier studies. For example, in the present study, the dynamic Smagorinsky model predicts that the Smagorinsky model coefficient  $C_s$  (which is the square-root of dynamic model coefficient  $C$ ) should be about 0.165. This is very close to the value of 0.17 suggested by Lilly (1966) for homogeneous isotropic turbulence with cutoff in the inertial subrange. It is noteworthy that determining the model coefficient using the dynamic Smagorinsky model may have some limitations. This model predicts its model coefficient to be negative for a long period of time in the earlier transitional stage. Even this period of time increases with increasing initial Reynolds number. Obviously it leads to numerical instability. To prevent this problem from happening, we impose the constraints that  $C$  should be always larger than 0.01. This kind of numerical instability was not brought about by the other models.

Fig 3a shows contours of the SGS kinetic energy on  $32 \times 32 \times 32$  grid directly obtained by LES using the dynamic  $k$ -equation model. This result is compared to the prediction by the LES using the same model but different resolution,  $16 \times 16 \times 16$  grid, (Fig. 6b) at an arbitrary (but same) slice of the 3D field. The comparison shows that there is significant similarity between two LES results of different grid widths and thus confirms the self consistency of the dynamic  $k$ -equation model. The peak values of the coarser grid ( $16 \times 16 \times 16$ ) results are approximately twice of those from the finer grid ( $32 \times 32 \times 32$ ). This is reasonable because the coarser grid which has the lower cutoff wave number should contain the larger SGS kinetic energy inside of its subgrid regions for the same Reynolds number.

#### 4. FUTURE WORK TO BE INCLUDED IN THE FINAL PAPER

The results obtained so far show that the dynamic models that do not assume local equilibrium between the SGS energy production and dissipation rate perform significantly better than the dynamic model based on the classical Smagorinsky's eddy viscosity model. Further simulations are underway to confirm this result using finer grid resolution and for higher Reynolds numbers. Comparison of the LES results with the DNS results for representative (relatively low Reynolds numbers) cases will also be carried out. Finally, these models will be evaluated for different flow cases. For example, the Taylor-Green vortex flow, which has been used by Domaradzki *et al.* (1993), is considered a good test problem. This is, due to flow symmetry, a flow at a relatively high Reynolds number can be simulated using relatively coarse resolution. The results of these studies will be described in more details in the final paper.

## REFERENCES

- J. A. Domaradzki, W. Liu, and M. E. Brachet (1993), "An analysis of subgrid-scale interactions in numerically simulated isotropic turbulence," *Phys. Fluids A* 5, 1747.
- M. Germano, U. Piomelli, P. Moin, and W.H. Cabot (1991), "A dynamic subgrid-scale eddy viscosity model," *Phys. Fluids A* 3, 1760.
- D. K. Lilly (1966), "On the application of the eddy viscosity concept in the inertial sub-range of turbulence," NCAR Manuscript 123, National Center for Atmospheric Research, Boulder, CO.
- D. K. Lilly (1992), "A proposed modification of the Germano subgrid-scale closure method," *phys. Fluids* 4, 633.
- S. Menon and P. K. Yeung (1994), "Analysis of subgrid models using direct and large eddy simulations of isotropic turbulence," presented at the 74th AGARD/FDP Symposium on Application of Direct and Large Eddy Simulation to Transition and Turbulence, Chania, Greece, April 18-21, 1994.
- P. Moin, K. Squires, W. Cabot, and S. Lee (1991), "A dynamic subgrid-scale model for compressible turbulence and scalar transport," *Phys. Fluids A* 3, 2746.
- P. Moin, D. Carati, T. Lund, S. Ghosal, and K. Akselvoll (1994), "Developments and applications of dynamic models for large eddy simulation of complex flows," presented at the 74th AGARD/FDP Symposium on Application of Direct and Large Eddy Simulation to Transition and Turbulence, Chania, Greece, April 18-21, 1994.
- U. Piomelli, W. H. Cabot, P. Moin, and S. Lee (1991), "Subgrid-scale backscatter in turbulent and transitional flows," *Phys. Fluids A* 3, 1766.
- U. Piomelli (1993), "High Reynolds number calculations using the dynamic subgrid-scale stress model," *Phys. Fluids A* 5, 1484.
- U. Piomelli and J. Liu (1994), "Large-eddy simulation of rotating channel flows using a localized dynamic model," presented at the 74th AGARD/FDP symposium on Application of Direct and Large Eddy Simulation to Transition and Turbulence, Chania, Greece, April 18-21, 1994.

M.M. Rai and P. Moin (1991), "Direct simulations of turbulent flow using finite-difference schemes," *J. Comput. Phys.* 96, 15.

R. S. Rogallo (1981), "Numerical experiments in homogeneous turbulence," NASA Tech. Memo. 81315.

S. E. Rogers, D. Kwak, and C. Kiris (1991), "Steady and unsteady solutions of the incompressible Navier-Stokes equations," *AIAA J.* 29, 603.

V. C. Wong and D. K. Lilly (1994), "A comparison of two dynamic subgrid closure methods for turbulent thermal convection," *Phys. Fluids* 6, 1016.

K.-S. Yang and J. H. Ferziger (1993), "Large-eddy simulation of turbulent obstacle flow using a dynamic subgrid-scale model," *AIAA J.* 31, 1406.

A. Yoshizawa (1993), "Bridging between eddy-viscosity-type and second-order models using a two-scale DIA," presented at the 9th symposium on Turbulent Shear Flows, Kyoto, Japan, August 16-18, 1993.

Y. Zang, R.L. Street, and J.R. Koseff (1992), "Application of a dynamic subgrid-scale model to turbulent recirculating flows," in *CTR Annual Research Briefs 1992* (Center for Turbulence Research, Stanford University/NASA Ames, 1992), p. 85.

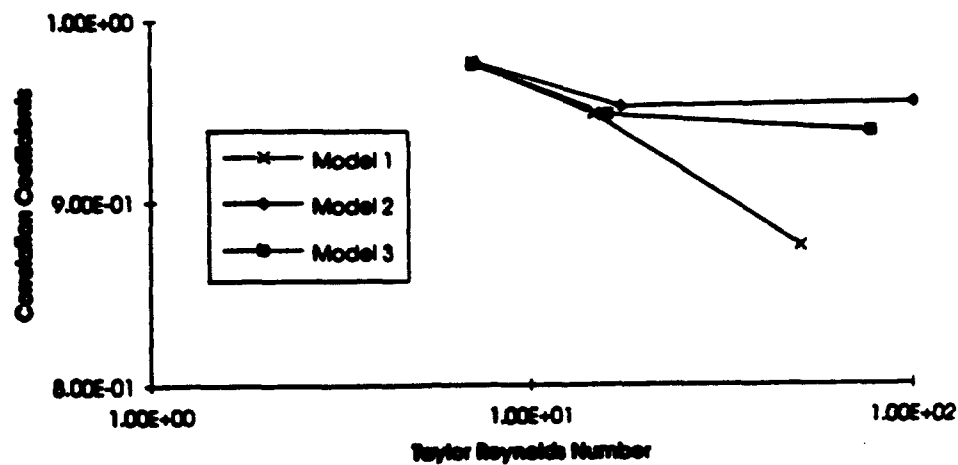


FIG. 1. Correlation between the LES results on 32x32x32 grid and on 16x16x16 grid as a function of the Taylor Reynolds number at the instant of the comparison.

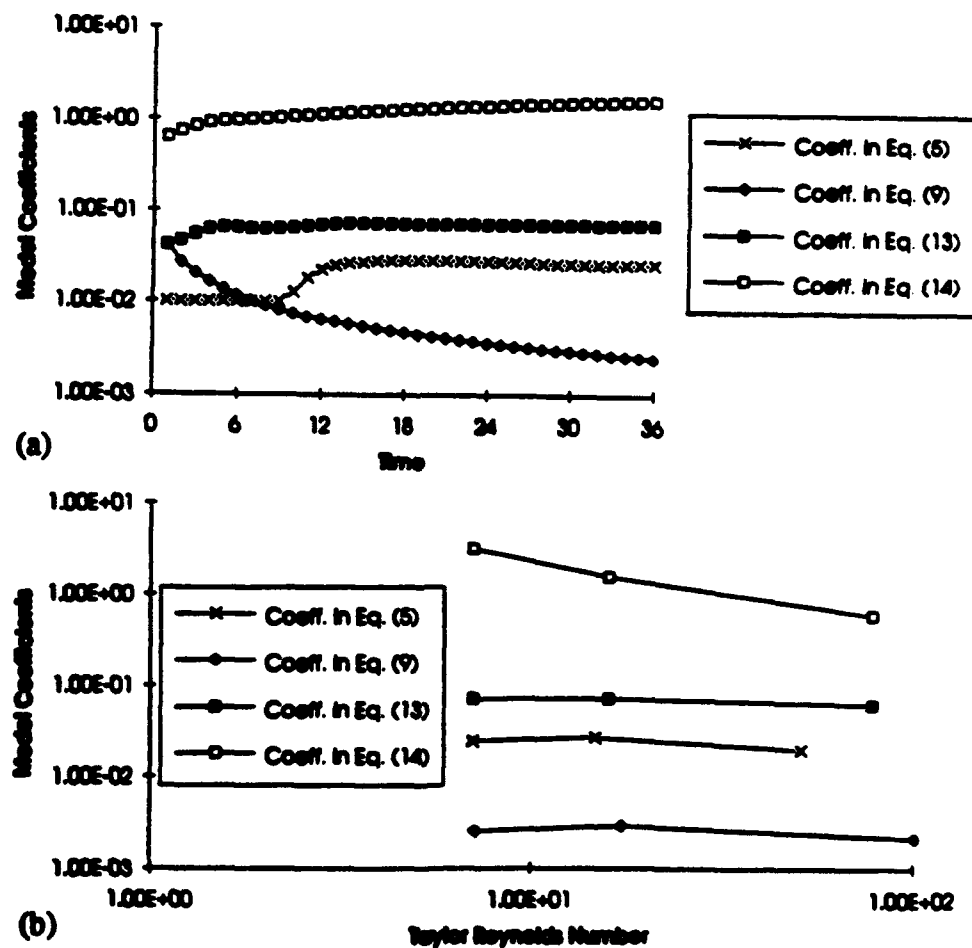
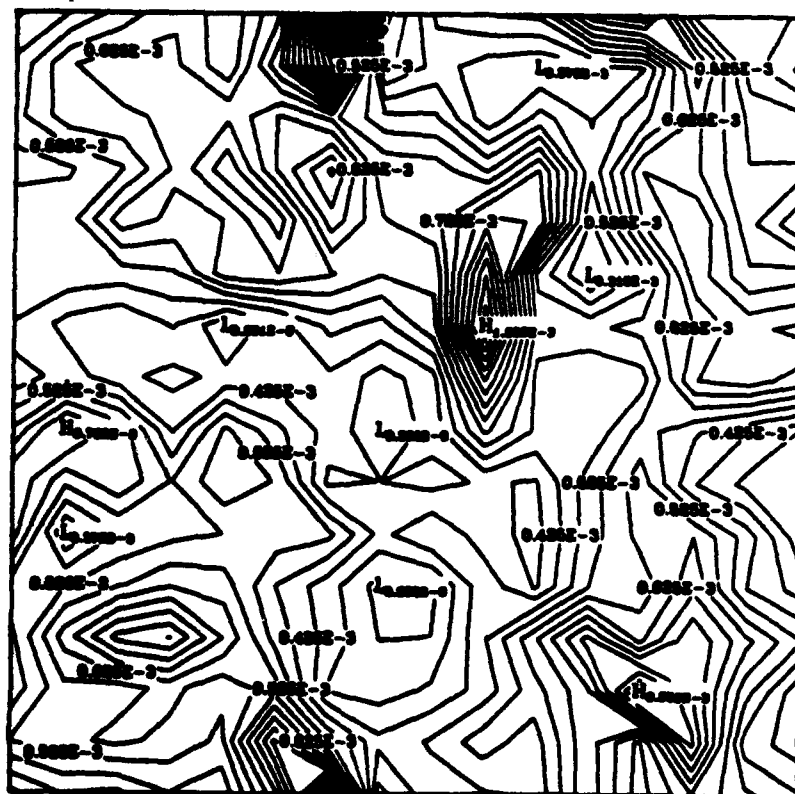


FIG. 2. Variation of the dynamically determined model coefficients: (a) as a function of time,  $Re_\lambda=100$ ; (b) as a function of the Taylor Reynolds number.



(a)

CONTOUR FROM 0.300E-4 TO 6.301E-4 BY 0.25E-4



(b)

CONTOUR FROM 0.250E-3 TO 1.375E-3 BY 0.06E-3

FIG. 3. Comparison of the contours of the SGS kinetic energy from two different LES using the dynamic  $k$ -equation model: (a) LES on 32x32x32 grid; (b) LES on 16x16x16 grid.